Jurassic to Early Cretaceous subduction-related magmatism in the Coastal Cordillera of northern Chile (18°30'-24°S): geochemistry and petrogenesis

Verónica Oliveros
Diego Morata
Luis Aguirre

Departamento de Geología, Universidad de Chile, Casilla 13518, Correo 21, Santiago, Chile
volivero@ing.uchile.cl
dmorata@ing.uchile.cl
luaguirr@ing.uchile.cl

Gilbert Féraud
Michel Fornari

UMR 6526 Géosciences Azur, IRD-CNRS-UNSA, Université de Nice- Sophia Antipolis, 06108 Nice cedex 02, France
feraud@unice.fr
fornari@unice.fr

ABSTRACT

Jurassic to Early Cretaceous magmatism in the Coastal Cordillera of northern Chile is represented by thick sequences of mostly basaltic-andesitic to andesitic lava flows and minor sedimentary rocks. The volcanic sucession was intruded by large plutonic bodies and smaller stocks and dikes. New geochemical data, including major and trace elements for a suite of Middle to Upper Jurassic volcanic and plutonic rocks from six localities in the Coastal Cordillera (18°30'-24°S), are presented here. The volcanic rocks are characterized by their petrological and chemical homogeneity; they are highly porphyritic basaltic-andesites and andesites with calc-alkaline to high-K calc-alkaline affinities, higher LILE than HFSE abundances, negative Nb and Ti anomalies, and LREE/HREE fractionation, which are the typical compositional features of subduction-related igneous rocks. No significant differences are observed in rocks from different areas or ages, but the plutonic rocks show subparallel, less and more enriched patterns respectively compared to volcanic rocks. The evolution and differentiation of the parental magmas is mainly due to fractional crystallization dominated by plagioclase, olivine and clinopyroxene. Assimilation of the continental crust was not important, although Th and La contents would indicate increasing sediment contribution or crustal contamination of the magmas with time. The magma source is likely to be a depleted mantle metasomatized by fluids, which originated from dehydration of the subducted oceanic crust. No evidence of slab melting was found in the studied rocks. The extensional tectonic setting that dominated the evolution of the Jurassic-Early Cretaceous arc in northern Chile would have favoured the extrusion of huge amounts of volcanic rocks during a relatively short period of time, avoiding thus a mayor interaction with the continental crust.

Key words: Geochemistry, Subduction, Jurassic, Chile.

RESUMEN

Magmatismo asociado a subducción del Jurásico a Cretácico Inferior en la Cordillera de la Costa del norte de Chile (18°30'-24°S): geoquímica y petrogénesis. En la Cordillera de la Costa del norte de Chile, el magmatismo del Jurásico y Cretácico Inferior está representado por potentes secuencias de rocas volcánicas y volcanoclásticas, principalmente de composición intermedia, y rocas sedimentarias. Ellas están intruidas por grandes plutones, además de diques e intrusivos menores. En este trabajo se presentan nuevos datos geoquímicos, de elementos mayores y traza, correspondientes a un grupo de rocas volcánicas y plutónicas del Jurásico Medio a Superior recogidas en seis localidades en la Cordillera de la Costa del norte de Chile (18°30'-24°S). Las rocas volcánicas

son bastante homogéneas en sus características petrográficas y geoquímicas y corresponden a lavas porfiríticas de composición basáltico-andesítica a andesítica, de afinidad calcoalcalina a calcoalcalina de alto-K, presentando mayor abundancia de elementos LIL con respecto a elementos HFS y anomalías negativas de Nb y Ti. Todos estos rasgos geoquímicos son típicos de rocas generadas en ambientes de subducción. No se observan diferencias significativas entre rocas volcánicas de distintas regiones o edades. Sin embargo, las rocas plutónicas presentan patrones de REE más planos, levemente más enriquecidos o empobrecidos, con respecto a los de las rocas volcánicas. La evolución y diferenciación de los magmas parentales se debió principalmente a la cristalización fraccionada de plagioclasa, olivino y clinopiroxeno sin una asimilación importante de corteza continental. Sin embargo, los contenidos de La y Th indicarían un aumento de la contribución de los sedimentos subductados en la génesis de los magmas o un aumento del grado de contaminación cortical con el tiempo. La fuente magmática fue posiblemente un manto deprimido, posteriormente metasomatizado por fluidos provenientes de la deshidratación de la placa subducida. No se encontraron evidencias geoquímicas de fusión de la corteza oceánica en las rocas estudiadas. El régimen tectónico extensional que dominó la evolución del arco magmático del Jurásico y Cretácico Inferior en el norte de Chile habría favorecido la extrusión de grandes volúmenes de rocas volcánicas en un período de tiempo relativamente corto, evitándose así la interacción de los magmas con la corteza continental.

Palabras claves: Geoquímica, Subducción, Jurásico, Chile.

INTRODUCTION

Huge amounts of volcanic and plutonic rocks from the Coastal Cordillera of northern Chile are related to the Jurassic-Lower Cretaceous magmatic arc which is thought to represent the first stages of the Andean subduction. The Jurassic-Lower Cretaceous arc would have been developed in an extensional to transtensional tectonic regime due to a variably oblique subduction of the Phoenix plate under the South American Plate at the western margin of Gondwana (Jaillard *et al.*, 1990; Scheuber and González, 1999; Grocott and Taylor, 2002). The development of the arc is characterized by a long lasting (~100 Ma) plutonic activity and a relatively short (15 to 25 Ma) volcanic activity (Oliveros *et al.*, 2006), the latter is represented by the extrusion of thick sequences of mainly intermediate lava flows. The end of magmatic activity in the Coastal Cordillera would be the result of an eastward migration of the arc during the Cretaceous and Cenozoic until it reached its present day position in the Andean Cordillera (Mpodozis and Ramos, 1989).

Although many authors agree that the volcanic and plutonic rocks cropping out in the Coastal Cordillera were originated from likely depleted mantle-derived magmas, the geological setting of the magmas has been interpreted in various ways, *e.g.,* an island-arc environment (Palacios, 1978), a back-arc setting in an active continental margin (Buchelt and Tellez, 1988; Rogers and Hawkesworth, 1989), magmatism triggered from decompressional melting of the lithospheric mantle without subduction-processes involved (Lucassen *et al.*, 1996) and magmatism controlled by pull-apart structures linked to oblique subduction (Pichowiak, 1994). All these models were established mainly by geochemical and petrological evidence from the Coastal Cordillera between 22° and 25°S. An arc/back-arc setting was proposed in the Arica and Iquique areas (18°30'-21°30); a westward migration of the arc and slab melt contribution to the magmas at the beginning in the Middle Jurassic and at the end in the Late Jurassic of the magmatic activity as a result of changes in the tectonic regime and subduction rate was proposed for this area (Kramer *et al.*, 2005).

These models are supported by variable amounts of geological, geochemical and geophysical data but rely on scarce age constraints, since the age of the volcanic units from the Coastal Cordillera has been largely unknown, with the exception of the Iquique region where the stratigraphic record is important. In this paper we present new geochemical data (major and trace elements) of recently dated volcanic and plutonic rocks from the Coastal Cordillera of northern Chile, between 18°30' and 24°S (Oliveros *et al.*, 2006; Oliveros *et al.*, in press a, b), in order to 1) establish similarities and differences between the volcanic units along the Coastal Cordillera, and 2) constrain the magma sources of the igneous rocks, the tectonic setting for their emplacement, and the possible evolution of the magmas with time.

GEOLOGIC AND TECTONIC SETTING

The Coastal Cordillera of northern Chile, between 18°30' and 23°30' (700 km) is a major geomorphologic unit mainly consisting of Mesozoic volcanic, plutonic and sedimentary rocks (Fig. 1). During the Jurassic and Early Cretaceous a subduction-related magmatic arc system developed along the present day Coastal Cordillera; the resulting Jurassic volcanic and sedimentary units crop out as homoclinal sequences that can reach thicknesses of 7,000 to 10,000 meters (Buchelt and Tellez, 1988; Muñoz *et al.*, 1988). The volcanic rocks are represented by the Camaraca and Los Tarros formations (Arica area), Oficina Viz, Caleta Ligate and El Godo formations (Iquique area) and La Negra Formation (Tocopilla, Michilla Mantos Blancos, Baquedano and Antofagasta areas). They mainly consist of porphyritic lavas with phenocryst contents up to 25%. Volcanic breccias, tuffs and sedimentary rocks as well as epiclastic sandstone lenses are less abundant. Basaltic andesites and andesites are by far the main compositional types, although basalts, dacites and rhyolites (ignimbrites) have been reported from several areas (Boric *et al.*, 1990; Cortés, 2000; Kramer *et al.*, 2005). Large and widely distributed plutonic bodies (Coastal Batholith), gabbroic to granitic in composition, intrude the volcanic sequence, together with dikes and stocks. The volcanic and plutonic rocks have predominantly calc-alkaline affinity (Buchelt and Tellez, 1988; Rogers and Hawkesworth, 1989; Lucassen and Franz, 1994), however, tholeiitic affinities have also been found in basaltic-andesite lava flows and gabbro intrusives, representing either initial stages of the arc evolution (Palacios, 1978; Pichowiak *et al.*, 1990; Lucassen and Franz, 1994) or a back-arc setting (Kramer *et al.*, 2005). The Sr-Nd-Pb isotopic compositions of volcanic and plutonic rocks are uniform ($^{87}Sr/^{86}Sr$: 0.70290-0.70464; $^{143}Nd/^{144}Nd$: 0.51250-0.51280; $^{206}Pb/^{204}Pb$: 17.96-18.42; $^{207}Pb/^{204}Pb$:15.55-15.67; $^{208}Pb/^{204}Pb$: 37.83-38.44), and indicate a depleted mantle source for the magmas, though some assimilation of the Paleozoic crust could have occurred during the evolution of the arc (Roger and Hawkesworth, 1989; Lucassen *et al.*, 2002; Kramer *et al.*, 2005).

The age of volcanism has traditionally been established on the basis of contact relationship with sedimentary units or the fossiliferous content of interbedded sediments, from Early to earliest Late Jurassic. Nevertheless, recent $^{40}Ar/^{39}Ar$ dating indicate that volcanism took place mainly between 165 and 150 Ma (Oxfordian-Kimmeridgian, ISC 2004) (Oliveros *et al.*, 2006), with a probable older episode at 170-175 Ma (Aaleninan-Early Bajocian; ISC, 2004) in the Iquique area (Kramer *et al.*, 2005; Oliveros *et al.*, 2006, Table 1).

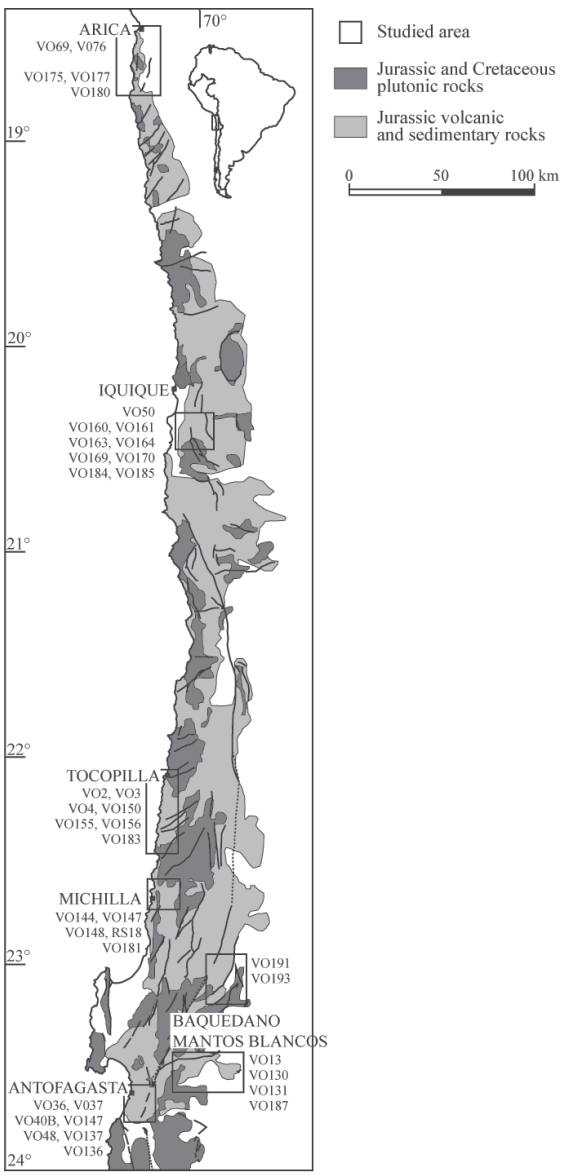

FIG. 1. Simplified geological map of the Coastal Cordillera of northern Chile (modified after SERNAGEOMIN, 2002) showing the sample locations.

TABLE 1a. INVESTIGATED SAMPLES AND THEIR LOCATION, TYPE, MINERALOGY AND AGE.

Sample No.	Coordinates		Age [Ma ± 2σ]		Rock type	Composition	Mineralogy
Arica area (Camaraca Formation)							
VO69	18°28'45"	70°19'28"	157.9 ± 0.8 (1)	P	Lava flow	andesite	pl, cpx, mag
VO76	18°32'46"	70°19'46"	159.2 ± 0.6 (1)	P	Lava flow	andesite	pl, cpx, mag
VO175	18°4614"	70°15'25"	157.2 ± 0.7 (1)	W	Lava flow	andesite	pl, cpx, mag
VO177	18°45'17"	70°20'06"	⩾157	S	Lava flow (SA)	basaltic andesite	pl, cpx, mag, ol*
VO180	18°45'21"	70°20'09"	⩾157	S	Lava flow	basaltic andesite	pl, cpx, mag, ol*
Iquique area (Oficina Viz Formation)							
VO50	20°27'00"	69°59'10"	~170-175	S	Lava flow	andesite	pl, cpx, mag
VO160	20°24'37"	70°00'41"	170.3 ± 3.0 (1)	W	Lava flow	andesite	pl, cpx, mag
VO161	20°24'37"	70°00'41"	146.0 ± 1.0 (1)	P	Dyke	dacite	pl, cpx, mag
VO163	20°24'38"	70°00'41"	175.8 ± 3.4 (1)	W	Lava flow	andesite	pl, cpx, mag
VO164	20°24'38"	70°00'41"	⩾ ~170-175	S	Lava flow	andesite	pl, cpx, mag
VO169	20°24'18"	69°58'03"	⩾161.4 ± 4.9 (1)	W	Lava flow	andesite	pl, cpx, mag
VO170	20°24'17"	69°58'04"	155.8 ± 5.1 (1)	W	Lava flow	basaltic andesite	pl, cpx, mag, ol*
VO184	20°28'01"	70°01'57"	~144	S	Intrusive	granite	pl, qtz, Kfs, hbl, bt, mag
VO185	20°28'02"	70°02'03"	144.4 ± 0.4 (1)	P	Intrusive	granodiorite	pl, qtz, Kfs, hbl, bt, mag
Tocopilla area (La Negra Formation)							
VO2	22°20'45"	70°14'48"	161.2 ± 1.1 (1)	P	Lava flow	andesite	pl, cpx, mag
VO3	22°05'31"	70°08'07"	155.6 ± 1.4 (1)	P	Intrusive	granodiorite	pl, qtz, Kfs, cpx, mag
VO4	22°08'47"	70°13'07"	164.9 ± 1.7 (1)	P	Lava flow	andesite	pl, cpx, mag
VO150	22°19'32"	70°14'53"	160.1 ± 1.5 (1)	P	Lava flow	andesite	pl, cpx, mag
VO155A	22°09'58"	70°12'09"	~161	S	Lava flow (SA)	basaltic andesite	pl, cpx, mag, ol*
VO156	22°09'58"	70°12'11"	160.2 ± 1.2 (1)	W	Lava flow	basaltic andesite	pl, cpx, mag, ol*
VO183	22°27'00"	70°15'29"	157.3 ± 0.8 (1)	P	Intrusive	diorite	pl, qtz, Kfs, cpx, hbl, mag
Michilla area (La Negra Formation)							
VO144	22°41'29"	70°14'02"	~160	S	Lava flow (SA)	basaltic andesite	pl, cpx, mag, ol*
VO147	22°41'28"	70°14'08"	~160	S	Lava flow	andesite	pl, cpx, mag, ol*
VO148	22°41'35"	70°14'13"	159.9 ± 1.0 (2)	P	Lava flow	basaltic andesite	pl, cpx, mag
VO181	22°43'32"	70°14'13"	159.6 ± 0.7 (2)	P	Intrusive	diorite	pl, qtz, Kfs, hbl, cpx, mag
RS18	22°4044"	70°10'03"	157.0 ± 5.0 (2)	S	Small intusive	diorite	pl, cpx, opx, mag
Mantos Blancos - Baquedano area (La Negra Formation)							
VO13	23°29'07"	70°08'38"	~156	S	Lava flow	andesite	pl, cpx, mag
VO130B	23°29'59"	70°03'24"	156.6 ± 1.4 (3)	P	Lava flow	andesite	pl, cpx, mag
VO131B	23°29'59"	70°03'24"	~156	S	Lava flow	andesite	pl, cpx, mag
VO187	23°30'41"	69°54'29"	161.5 ± 1.5 (3)	P	Lava flow (SA)	basaltic andesite	pl, cpx, mag, ol*
VO191	23°04'53"	69°56'11"	~150	S	Lava flow	andesite	pl, cpx, mag
VO193	23°04'48"	69°57'30"	150.2 ± 2.8 (3)	W	Lava flow	basaltic andesite	pl, cpx, mag, ol*
Antofagasta area (La Negra Formation)							
VO36A	23°41'46"	70°23'45"	150.1 ± 0.7 (1)	P	Lava flow	basaltic andesite	pl, cpx, mag, ol*
VO37	23°42'31"	70°22'57"	152.0 ± 1.0 (1)	P	Lava flow	basaltic andesite	pl, cpx, mag, ol*
VO40B	23°44'59"	70°21'03"	157.4 ± 0.8 (1)	W	Lava flow	andesite	pl, cpx, mag
VO48	23°45'06"	70°20'25"	154.7 ± 1.0 (1)	W	Lava flow	andesite	pl, cpx, mag
VO47	23°45'11"	70°20'52"	~155	S	Lava flow (SA)	basaltic andesite	pl, cpx, mag, ol*
VO137	23°37'06"	70°18'07"	154.7 ± 2.4 (1)	W	Lava flow	andesite	pl, cpx, mag
VO142	23°37'19"	70°20'05"	~152	S	Lava flow	andesite	pl, cpx, mag
VO136	23°35'56"	70°17'22"	153.4 ± 0.8 (1)	P	Intrusive	granite	pl, qtz, Kfs, hbl, bt, mag

TABLE 1b

Lava flow	Mineralogy	Texture	Alteration
Phenocrysts	Plagioclase (60-100%)	Euhedral/subhedral	Partially altered to sericite and minor
(0-25%)	$An_{67-49}Ab_{49-31}Or_{3-1}$ normal zoning	0.5-2 cm Partially albitized	chlorite, pumpellyite, prehnite, epidote.
	Clinopyroxene (0-40%) $En_{53-34}Fs_{28-11}Wo_{49-27}$	Euhedral/subhedral 1-5mm	Partially altered to chlorite and titanite.
	Olivine (0-10%) <5mm	Idiomorphic euhedral	Completely altered to iddignsite and chlorite, minor quartz.
	Fe-Ti oxides (<5%) <2mm	Euhedral/subhedral	Partially altered to titanite.
Groundmass (75-100%) Glass	Plagioclase, Fe-Ti oxides Clinopyroxene	Intersertal Intergranular	Glass is crystallized to titanite, chlorite and Fe-Ti oxides (except VO69 VO76. VO40B). Altered to calcite, epidote, actinolite (VO47), pumpellyite (VO164), quartz.

1- Oliveros *et al.,* 2006; **2-** Oliveros *et al.,* in press(a); **3-** Oliveros *et al.,* in press(b). **P**: plateau $^{40}Ar/^{39}Ar$ age; **W**: weighted mean $^{40}Ar/^{39}Ar$ age (less than 70% of gas released), **S**: suggested age (normally inferred by its proximity to a dated sample). **Pl**: plagioclase, **cpx**: clinopyroxene, **opx**: orthopyroxene, **ol***: olivine (pseudomorph), **mag**: magnetite; **qtz**: quartz, **Kfs**: potassic feldspar, **hbl**: hornblende, **bt**: biotite. **SA**: strongly altered rock, **CM**: rock underwent contact metamorphism.

Plutonic rocks belonging to the Coastal Batholith and several dikes have been dated by K-Ar, U-Pb, $^{40}Ar/^{39}Ar$, and Sm-Nd methods. The ages range from *ca.* 106 and 200 Ma, apparently showing two phases of magmatic activity and a possible gap between *ca.* 160 and 170 Ma (Maksaev, 1990; Andriessen and Reutter, 1994; Pichowiak, 1994; Scheuber *et al.* 1995; Dallmeyer *et al.*, 1996; Lucassen and Thirlwall 1998; Cortés, 2000; Basso, 2004; González and Niemeyer, 2005; Cortés *et al.*, in press; Oliveros *et al.*, 2006; Oliveros *et al.* in press a, b). Therefore, volcanism and the second phase of plutonism (*ca.* 160-106 Ma) were at least partly contemporaneous.

Structural and geochemical studies carried out between 23°S and 28°S suggest that throughout the Jurassic and Early Cretaceous, the subduction system developed under an extensional and later transtensional tectonic regime (Scheuber and González, 1999). The arc itself accommodated most of the deformation, as evidenced by the structures observed in syn-tectonic plutonic bodies that intruded at relative deep crustal levels, whereas tectonic quiescence dominated in the back-arc basins located farther to the east (Prinz *et al.*, 1994; Scheuber and González, 1999; Grocott and Taylor, 2002). The shift from extensional to transtensional regime occurred likely at the Jurassic-Cretaceous boundary (Scheuber and González, 1999; Grocott and Taylor, 2002) after the deposition of the whole volcanic sequence (Oliveros *et al.*, 2006) and the later activation of the Atacama Fault System (AFS), a 1000 km trench-parallel structure that accommodated strike-slip displacements, at ~135-120 Ma. The magmatic arc and fault system were abandoned after *ca.* 118 to 106 Ma, the magma foci shifted to the east and a compressive tectonic regime started during the Late Cretaceous (Grocott and Taylor, 2002; Cembrano *et al.,* 2005).

Both volcanic and sedimentary units are largely affected by several hydrothermal alteration and/or non-deformational metamorphism processes that likely occurred between 160 and 100 Ma. Some of these processes were partially contemporaneous with the extrusion of volcanics and the emplacement of large and small plutonic bodies (Losert, 1974; Oliveros, 2005). Stratabound and breccia-style Cu (±Ag) deposits, hosted in volcanic rocks, together with vein-type Cu deposits hosted in plutonic rocks are mayor economic deposits in the region. Hydrothermal alteration processes accompanied the generation of these deposits, also resulting in the formation of secondary mineral phases (Losert, 1974; Oliveros *et al.*, 2003).

ANALYTICAL METHODS AND PETROGRAPHIC CHARACTERIZATION OF THE STUDIED SAMPLES

Forty samples of volcanic and plutonic rocks were selected for major, trace and rare earth elements chemical analyses. Samples of volcanic rocks containing amygdales and veinlets were avoided except for 6 strongly altered lavas, one for each studied area, analyzed in order to evaluate the impact of alteration. The analyses were carried out by ICP-AES and ICP-MS at the Centre de Recherches Pétrographiques et Géochimiques, Vandœuvre les Nancy (France). Uncertainties are under 2% for major elements and under 5% for trace and rare earth elements, except for Co, Cs, Hf, Ho, Ni, Rb, Th and Tm, with uncertainties under 10%. Chemical compositions of plagioclase and pyroxene phenocrysts were obtained using a CAMECA SX-100 electron microprobe with 20kV, 0,001 nA and 2-5 μm as analytical conditions, at the Institut des Sciences de la Terre de l'Environnement et de l'Espace of the Université de Montpellier (France).

The studied volcanic rocks correspond exclusively to lava flows from the Camaraca (Arica area), Oficina Viz (Iquique area) and La Negra (Tocopilla, Michilla, Mantos Blancos-Baquedano and Antofagasta areas) formations (Fig. 1). These flows are 1 to 10 m in thickness and present a typical morphology with an amygdaloidal bottom, a massive center with porphyritic or aphyric texture and a more altered brecciated top with high amygdale content. Plagioclase, clinopyroxene, idiomorphic olivine, and Fe-Ti oxides (magnetite) and a microcrystalline matrix (former glass) are the mineralogical components of the lavas (Table 1a). Phenocrysts are more abundant in the massive centers whereas glass predominates in the top and bottom of the flows.

The plagioclase phenocrysts composition is labradorite ($An_{67-49}Ab_{49-31}Or_{3-1}$) and is rather homogeneous for rocks of all studied areas (Table 2, Fig.

2a); rims are normally less calcic than cores (An_{49-55} *versus* An_{55-67}) as a consequence of magmatic zonation and not because of Ca-loss due to alteration. Clinopyroxene phenocrysts are predominantly augite ($En_{53-34}Fs_{28-11}Wo_{49-27}$), although some pigeonite is found in recrystallized rims of these phenochrysts; the Ti-Ca contents correspond to those of calc-alkaline basalts (Table 3, Fig. 2b,c). The groundmass is composed by plagioclase microlites, normally flux-oriented near the bottom and tops of the lava flows, clinopyroxenes, Fe-Ti oxides and crystallized glass, its texture is intersertal or intergranular (Table 1b).

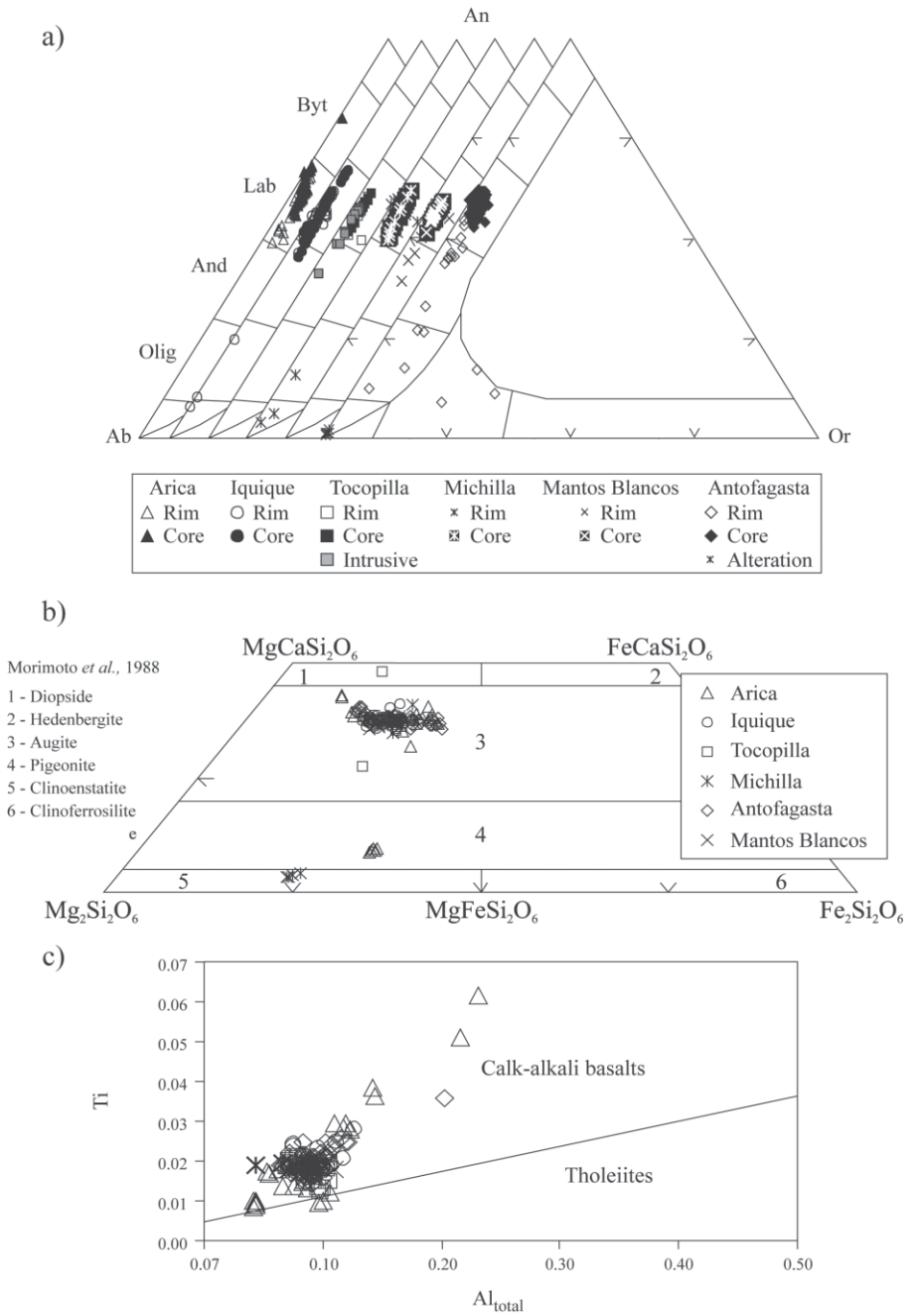

FIG. 2. **a-** Classification diagram for plagioclase phenocrysts; **b-** classification diagram for pyroxene phenocrysts (Morimoto *et al.*, 1988); **c-** discrimination diagram for clinopyroxene phenocrysts (Leterrier *et al.*, 1982), from the different studied areas.

TABLE 2. MEAN VALUES AND STANDARD DEVIATION (1σ) FOR MICROPROBE ANALYSES OF PLAGIOCLASE PHENOCRYSTS. STRUCTURAL FORMULAE ON THE BASIS OF 8 OXYGENS.

Locality	Arica												Iquique																	
Sample	VO69				VO76				VO175				VO180				VO50				VO160				VO163				VO169			
	rim		core		rim		core		rim		core		rim		core		rim		core		rim		core		rim		core		rim		core	
No. of analyses	9	± 1σ	11	± 1σ	7	± 1σ	11	± 1σ	10	± 1σ	14	± 1σ	11	± 1σ	14	± 1σ	14	± 1σ	22	± 1σ	13	± 1σ	20	± 1σ	10	± 1σ	14	± 1σ	10	± 1σ	11	± 1σ
SiO_2	53.97	0.90	53.86	0.78	54.53	1.16	53.35	1.53	54.41	3.92	53.22	0.47	52.90	1.37	50.93	0.62	55.28	0.68	55.44	0.65	53.58	0.86	53.85	0.74	57.70	4.92	53.75	0.79	53.21	0.65	53.19	0.84
TiO_2	0.07	0.01	0.06	0.02	0.08	0.01	0.07	0.02	0.13	0.12	0.07	0.02	0.07	0.02	0.05	0.02	0.10	0.02	0.10	0.01	0.07	0.01	0.08	0.02	0.06	0.04	0.08	0.01	0.07	0.01	0.07	0.02
Al_2O_3	28.77	0.81	28.83	0.45	28.53	0.71	29.25	1.31	27.08	4.52	29.02	0.23	28.90	1.12	30.36	0.43	28.17	0.30	27.86	0.47	28.77	0.24	28.73	0.34	26.09	3.15	28.02	1.27	28.81	0.39	28.69	0.64
FeO	0.95	0.10	0.87	0.03	1.00	0.07	0.94	0.07	1.16	0.47	0.87	0.02	0.93	0.16	0.74	0.08	0.74	0.03	0.73	0.04	0.84	0.11	0.79	0.02	0.78	0.52	0.82	0.08	0.92	0.08	0.91	0.04
MnO	0.01	0.01	0.01	0.01	0.01	0.00	0.01	0.01	0.02	0.02	0.01	0.01	0.01	0.01	0.01	0.01	0.01	0.01	0.00	0.01	0.01	0.01	0.01	0.01	0.01	0.01	0.01	0.01	0.00	0.01	0.02	0.01
MgO	0.13	0.03	0.12	0.01	0.13	0.02	0.13	0.02	0.33	0.35	0.12	0.01	0.19	0.27	0.16	0.02	0.12	0.01	0.12	0.01	0.14	0.02	0.14	0.01	0.14	0.18	0.13	0.02	0.13	0.03	0.12	0.02
CaO	12.12	0.82	12.19	0.42	11.92	0.72	12.69	1.29	10.70	4.00	12.34	0.28	11.87	1.28	13.66	0.45	11.03	0.36	10.94	0.52	12.04	0.52	12.03	0.35	8.65	4.01	11.58	1.19	11.77	0.94	12.21	0.96
Na_2O	4.34	0.40	4.31	0.23	4.53	0.41	4.10	0.65	3.93	0.51	4.35	0.20	4.55	0.55	3.74	0.24	5.28	0.22	5.32	0.26	4.39	0.33	4.00	0.72	6.59	2.48	4.82	0.41	4.63	0.20	4.70	0.36
K_2O	0.50	0.09	0.51	0.05	0.46	0.06	0.42	0.09	1.96	3.63	0.43	0.02	0.29	0.08	0.14	0.06	0.32	0.09	0.38	0.10	0.31	0.02	0.30	0.02	0.27	0.14	0.35	0.08	0.44	0.17	0.30	0.05
BaO	0.01	0.01	0.01	0.01	0.03	0.01	0.01	0.02									0.02	0.01	0.00	0.01												
Total	**100.89**	**0.40**	**100.80**	**0.60**	**101.22**	**0.66**	**101.00**	**0.63**	**99.73**	**1.17**	**100.45**	**0.23**	**99.72**	**0.90**	**99.81**	**0.41**	**101.07**	**0.52**	**100.92**	**0.53**	**100.15**	**1.48**	**99.94**	**1.35**	**100.28**	**1.91**	**99.55**	**2.18**	**100.01**	**0.84**	**100.22**	**0.88**
An	58.94	3.97	59.20	2.11	57.68	3.73	61.58	6.25	52.87	19.05	59.54	1.64	58.02	5.47	66.30	2.30	52.61	1.85	52.04	2.24	59.21	1.39	61.54	3.97	41.66	19.72	55.80	4.74	56.85	2.50	57.94	3.54
Ab	38.18	3.47	37.85	1.85	39.65	3.42	36.00	5.72	35.29	3.90	37.97	1.54	40.29	5.00	32.87	2.03	45.60	1.77	45.82	2.14	38.99	1.39	36.63	4.01	56.77	20.44	42.18	4.23	40.58	1.97	40.36	3.24
Or	2.89	0.53	2.95	0.28	2.66	0.32	2.42	0.54	11.84	21.65	2.49	0.13	1.69	0.47	0.83	0.36	1.79	0.49	2.14	0.55	1.80	0.12	1.83	0.09	1.57	0.83	2.02	0.51	2.58	1.09	1.71	0.31

Table 2 (continuation)

Locality	Tocopilla													Michilla																
Sample	VO170		VO2				VO3		VO4				VO150	VO156		VO31			VO148				VO147				RS18			
	rim	core	rim		core		core		rim		core		core	rim	core	rim		core	rim		core		rim		core		rim		core	
No. of analyses	5	5	9	± 1σ	11	± 1σ	10	± 1σ	9	± 1σ	11	± 1σ	6	4	6	14	± 1σ	19	± 1σ	11	± 1σ	14	± 1σ	7	± 1σ	8	± 1σ	9	± 1σ	13	± 1σ
SiO_2	53.51	53.26	55.38	0.82	54.81	0.90	55.54	1.17	54.16	0.98	54.19	0.55	56.08	56.38	54.18	53.94	1.00	54.19	1.17	55.40	2.70	54.46	0.36	60.55	5.52	55.94	1.35	57.34	4.20	53.68	1.26
TiO_2	0.08	0.09	0.08	0.02	0.07	0.01	0.07	0.01	0.07	0.02	0.07	0.01	0.07	0.07	0.08	0.07	0.01	0.07	0.01	0.07	0.02	0.08	0.01	0.05	0.04	0.08	0.02	0.07	0.02	0.07	0.02
Al_2O_3	27.97	28.29	27.98	0.37	28.16	0.57	28.62	0.95	28.87	0.22	28.71	0.24	27.86	27.43	28.58	27.89	0.64	28.06	0.39	28.52	1.27	29.18	0.32	24.80	3.45	27.52	1.20	26.48	1.74	28.92	1.14
FeO	1.03	0.96	0.80	0.03	0.82	0.04	0.37	0.05	0.99	0.04	0.98	0.02	0.86	0.85	0.91	0.99	0.23	0.87	0.03	1.04	0.51	0.92	0.03	0.52	0.37	1.26	1.36	0.54	0.14	0.87	0.69
MnO	0.01	0.00	0.01	0.01	0.00	0.00	0.01	0.01	0.01	0.00	0.01	0.01	0.01	0.01	0.00	0.01	0.01	0.01	0.01	0.03	0.06	0.01	0.01	0.02	0.03	0.01	0.01	0.01	0.02	0.01	0.01
MgO	0.24	0.14	0.10	0.02	0.09	0.01	0.01	0.01	0.14	0.02	0.13	0.02	0.09	0.10	0.11	0.16	0.13	0.10	0.01	0.26	0.50	0.12	0.01	0.08	0.05	0.26	0.42	0.05	0.05	0.20	0.56
CaO	10.60	11.51	10.92	0.57	11.56	0.68	10.93	1.07	12.09	0.33	12.07	0.34	10.90	10.24	12.05	11.05	1.57	11.27	0.56	10.67	3.38	12.32	0.31	5.85	5.22	9.74	1.80	8.23	2.05	11.42	1.09
Na_2O	4.90	4.79	5.07	0.22	4.90	0.34	5.25	0.61	4.48	0.19	4.51	0.14	5.24	5.32	4.59	4.66	0.24	4.68	0.16	4.73	0.49	4.35	0.15	7.72	2.88	4.86	0.45	6.80	0.96	4.81	0.47
K_2O	0.67	0.32	0.50	0.20	0.40	0.04	0.39	0.04	0.35	0.03	0.34	0.01	0.46	0.65	0.46	0.81	0.89	0.43	0.03	0.72	1.16	0.36	0.03	0.86	1.23	0.63	0.30	0.52	0.30	0.33	0.15
BaO			0.02	0.01	0.02	0.01	0.02	0.01	0.01	0.01	0.01	0.02				0.02	0.01	0.01	0.01												
Total	**99.02**	**99.35**	**100.87**	**0.54**	**100.86**	**0.75**	**101.25**	**0.54**	**101.18**	**1.08**	**101.05**	**0.77**	**101.57**	**101.05**	**100.96**	**99.61**	**1.91**	**99.70**	**1.76**	**101.43**	**2.04**	**101.78**	**0.32**	**100.46**	**1.91**	**100.28**	**2.07**	**100.05**	**1.87**	**100.32**	**0.66**
Si	2.45	2.44	2.49	0.03	2.47	0.03	2.48	0.05	2.43	0.02	2.44	0.01	2.50	2.52	2.44	2.46	0.03	2.46	0.02	2.47	0.09	2.43	0.01	2.69	0.21	2.52	0.03	2.58	0.13	2.43	0.05
Ti	0.00	0.00	0.00	0.00	0.00	0.00	0.00	0.00	0.00	0.00	0.00	0.00	0.00	0.00	0.00	0.00	0.00	0.00	0.00	0.00	0.00	0.00	0.00	0.00	0.00	0.00	0.00	0.00	0.00	0.00	0.00
Al	1.51	1.53	1.48	0.02	1.49	0.03	1.51	0.05	1.53	0.02	1.52	0.01	1.46	1.45	1.52	1.50	0.02	1.50	0.01	1.50	0.06	1.54	0.02	1.30	0.19	1.46	0.07	1.41	0.12	1.54	0.06
Fe^{2+}	0.04	0.04	0.03	0.00	0.03	0.00	0.01	0.00	0.04	0.00	0.04	0.00	0.03	0.03	0.03	0.04	0.01	0.03	0.00	0.04	0.02	0.03	0.00	0.02	0.01	0.05	0.05	0.02	0.01	0.03	0.03
Mn^{2+}	0.00	0.00	0.00	0.00	0.00	0.00	0.00	0.00	0.00	0.00	0.00	0.00	0.00	0.00	0.00	0.00	0.00	0.00	0.00	0.00	0.00	0.00	0.00	0.00	0.00	0.00	0.00	0.00	0.00	0.00	0.00
Mg	0.02	0.01	0.01	0.00	0.01	0.00	0.00	0.00	0.01	0.00	0.01	0.00	0.01	0.01	0.01	0.01	0.01	0.01	0.00	0.02	0.04	0.01	0.00	0.01	0.00	0.02	0.03	0.00	0.00	0.01	0.04
Ca	0.52	0.56	0.53	0.03	0.56	0.04	0.52	0.05	0.58	0.02	0.58	0.01	0.52	0.49	0.58	0.54	0.07	0.55	0.02	0.51	0.16	0.59	0.01	0.28	0.25	0.47	0.08	0.40	0.11	0.55	0.05
Na	0.44	0.42	0.44	0.02	0.43	0.03	0.45	0.05	0.39	0.01	0.39	0.01	0.45	0.46	0.40	0.41	0.02	0.41	0.02	0.41	0.04	0.38	0.01	0.66	0.24	0.42	0.03	0.59	0.08	0.42	0.04
K	0.04	0.02	0.03	0.01	0.02	0.00	0.02	0.00	0.02	0.00	0.02	0.00	0.03	0.04	0.03	0.05	0.05	0.02	0.00	0.04	0.07	0.02	0.00	0.05	0.07	0.04	0.02	0.03	0.02	0.02	0.01
Sum cations	5.02	5.02	5.00	0.01	5.01	0.01	5.00	0.01	5.00	0.01	5.00	0.01	5.01	5.00	5.01	5.01	0.03	5.00	0.01	5.00	0.05	5.00	0.00	5.01	0.02	4.98	0.04	5.03	0.06	5.02	0.01
An	52.44	56.03	52.76	2.40	55.32	3.16	52.33	5.21	58.69	1.51	58.48	1.35	52.08	49.77	57.64	53.85	5.85	55.64	1.76	52.11	14.77	59.76	1.38	28.04	25.04	50.17	5.11	38.87	9.29	55.65	4.51
Ab	43.67	42.14	44.38	1.93	42.42	2.93	45.43	5.21	39.30	1.38	39.56	1.31	45.30	46.51	39.74	41.32	2.24	41.84	1.67	43.15	8.11	38.17	1.25	66.77	23.78	45.84	3.20	58.20	8.18	42.45	4.18
Or	3.89	1.83	2.86	1.15	2.26	0.25	2.25	0.21	2.01	0.16	1.96	0.08	2.62	3.72	2.62	4.83	5.50	2.52	0.14	4.74	8.53	2.07	0.15	5.18	7.79	3.99	2.39	2.93	1.73	1.90	0.86

Table 2 (continuation)

Locality	Mantos Blancos - Baquedano				Antofagasta																							
Sample	VO130B				S24				VO36					VO37				VO40B				VO48				VO137			
	rim		core		rim		core		rim		core			rim		core		rim		core		rim		core		rim		core	
No. of analyses	**7**	**± 1σ**	**10**	**± 1σ**	**10**	**± 1σ**	**14**	**± 1σ**	**14**	**± 1σ**	**15**	**± 1σ**	**5**	**13**	**± 1σ**	**18**	**± 1σ**	**14**	**± 1σ**	**18**	**± 1σ**	**11**	**± 1σ**	**15**	**± 1σ**	**9**	**± 1σ**	**13**	**± 1σ**
SiO_2	53.99	1.10	53.73	0.69	55.73	1.81	55.14	0.45	56.83	5.74	54.04	0.53	69.00	58.73	5.65	55.14	0.51	55.62	2.51	54.24	0.91	55.14	1.95	53.87	0.44	53.25	0.67	53.35	0.41
TiO_2	0.07	0.01	0.07	0.01	0.11	0.02	0.11	0.01	0.08	0.01	0.07	0.01	0.01	0.06	0.03	0.08	0.01	0.07	0.01	0.08	0.01	0.08	0.01	0.06	0.01	0.09	0.03	0.09	0.01
Al_2O_3	28.35	0.65	28.45	0.46	28.18	1.02	28.55	0.24	26.82	4.40	28.75	0.38	20.27	25.23	3.05	28.42	0.30	28.08	1.12	28.65	0.36	28.21	1.04	28.82	0.27	28.69	1.61	29.11	0.26
FeO	0.91	0.06	0.84	0.03	0.80	0.11	0.75	0.03	0.91	0.20	0.92	0.02	0.03	1.74	3.59	0.85	0.03	0.95	0.15	0.88	0.03	1.02	0.15	0.98	0.08	0.86	0.32	0.76	0.03
MnO	0.01	0.01	0.01	0.01	0.01	0.01	0.01	0.01	0.01	0.01	0.01	0.01	0.01	0.04	0.11	0.01	0.01	0.05	0.08	0.01	0.01	0.01	0.01	0.01	0.01	0.02	0.01	0.00	0.01
MgO	0.15	0.06	0.14	0.02	0.11	0.03	0.12	0.01	0.16	0.10	0.11	0.01	0.00	0.98	2.78	0.10	0.02	0.26	0.28	0.12	0.01	0.08	0.02	0.13	0.02	0.21	0.11	0.16	0.02
CaO	10.74	1.11	11.62	0.52	10.87	1.28	11.51	0.26	9.96	4.17	12.14	0.37	0.28	7.06	4.06	11.53	0.28	9.47	4.06	12.04	0.34	11.27	1.39	12.35	0.38	11.46	1.58	12.18	0.29
Na_2O	4.69	0.59	4.65	0.26	5.19	0.68	4.89	0.11	4.45	0.89	4.40	0.23	11.40	6.09	1.94	4.77	0.15	4.76	1.12	4.48	0.19	5.02	0.75	4.48	0.16	4.27	0.49	4.53	0.18
K_2O	0.64	0.45	0.36	0.04	0.40	0.12	0.33	0.02	2.00	3.79	0.47	0.04	0.06	1.43	2.00	0.50	0.04	1.66	2.35	0.42	0.03	0.34	0.09	0.28	0.03	0.95	1.10	0.20	0.01
BaO									0.01	0.01	0.02	0.01	0.01	0.01	0.01	0.01	0.02	0.02	0.02	0.01	0.01	0.01	0.00	0.01	0.01				
Total	**99.58**	**0.60**	**99.87**	**0.19**	**101.39**	**0.73**	**101.41**	**0.62**	**101.24**	**0.45**	**100.92**	**0.29**	**101.09**	**101.38**	**1.33**	**101.44**	**0.51**	**100.93**	**1.00**	**100.94**	**0.93**	**101.18**	**0.57**	**101.01**	**0.53**	**99.82**	**1.34**	**100.40**	**0.23**
Si	2.46	0.04	2.44	0.03	2.49	0.06	2.46	0.01	2.55	0.24	2.44	0.02	2.98	2.61	0.20	2.47	0.01	2.50	0.10	2.44	0.02	2.47	0.07	2.43	0.01	2.43	0.03	2.41	0.02
Ti	0.00	0.00	0.00	0.00	0.00	0.00	0.00	0.00	0.00	0.00	0.00	0.00	0.00	0.00	0.00	0.00	0.00	0.00	0.00	0.00	0.00	0.00	0.00	0.00	0.00	0.00	0.00	0.00	0.00
Al	1.52	0.04	1.52	0.03	1.48	0.06	1.50	0.01	1.42	0.24	1.53	0.02	1.03	1.33	0.16	1.50	0.01	1.49	0.07	1.52	0.02	1.49	0.06	1.53	0.01	1.54	0.06	1.55	0.01
Fe^{2+}	0.03	0.00	0.03	0.00	0.03	0.00	0.03	0.00	0.03	0.01	0.03	0.00	0.00	0.07	0.15	0.03	0.00	0.04	0.01	0.03	0.00	0.04	0.01	0.04	0.00	0.03	0.01	0.03	0.00
Mn^{2+}	0.00	0.00	0.00	0.00	0.00	0.00	0.00	0.00	0.00	0.00	0.00	0.00	0.00	0.00	0.00	0.00	0.00	0.00	0.00	0.00	0.00	0.00	0.00	0.00	0.00	0.00	0.00	0.00	0.00
Mg	0.01	0.00	0.01	0.00	0.01	0.00	0.01	0.00	0.01	0.01	0.01	0.00	0.00	0.07	0.20	0.01	0.00	0.02	0.02	0.01	0.00	0.01	0.00	0.01	0.00	0.01	0.01	0.01	0.00
Ca	0.52	0.05	0.57	0.03	0.52	0.06	0.55	0.01	0.48	0.20	0.59	0.02	0.01	0.34	0.19	0.55	0.01	0.46	0.20	0.58	0.02	0.54	0.07	0.60	0.02	0.56	0.08	0.59	0.01
Na	0.41	0.05	0.41	0.02	0.45	0.06	0.42	0.01	0.39	0.08	0.38	0.02	0.95	0.52	0.15	0.41	0.01	0.41	0.09	0.39	0.01	0.44	0.06	0.39	0.01	0.38	0.04	0.40	0.02
K	0.04	0.03	0.02	0.00	0.02	0.01	0.02	0.00	0.11	0.21	0.03	0.00	0.00	0.08	0.11	0.03	0.00	0.10	0.14	0.02	0.00	0.02	0.01	0.02	0.00	0.06	0.07	0.01	0.00
Sum cations	5.00	0.02	5.01	0.00	5.00	0.00	5.00	0.00	4.99	0.06	5.00	0.01	4.98	5.02	0.08	5.00	0.01	5.01	0.01	5.00	0.01	5.01	0.00	5.01	0.01	5.01	0.02	5.01	0.01
An	53.68	4.52	56.80	2.51	52.43	6.19	55.48	0.96	48.04	20.02	58.78	1.96	1.36	35.08	18.45	55.54	1.40	46.18	18.80	58.35	1.67	54.29	6.88	59.41	1.58	56.22	5.48	59.05	1.38
Ab	42.41	4.51	41.12	2.29	45.27	5.67	42.62	0.90	39.20	6.66	38.54	1.76	98.31	55.98	14.46	41.61	1.22	43.02	11.19	39.25	1.50	43.74	6.36	38.98	1.43	38.17	4.72	39.77	1.34
Or	3.91	3.01	2.08	0.22	2.30	0.69	1.90	0.10	12.76	25.10	2.69	0.21	0.33	8.94	12.74	2.85	0.21	10.80	16.59	2.40	0.18	1.97	0.52	1.61	0.16	5.61	6.63	1.18	0.07

TABLE 3. MEAN VALUES AND STANDARD DEVIATION (1σ) FOR MICROPROBE ANALYSES OF PYROXENE PHENOCRYSTS. STRUCTURAL FORMULAE ON THE BASIS OF 6 OXYGENS. FE^{3+}/FE^{2+} CALCULATIONS ACCORDING TO DROOP (1987).

Locality	Arica						Iquique						Tocopilla								Michilla		Mantos Blancos - Baq.				Antofagasta							
Sample	VO69		VO70		VO76		VO175		VO177		VO169		VO170		VO2		VO4		VO156		VO155A	RS18			VO130B		VO131B		VO36A		VO37		VO40B	VO48		VO137	
No. of analyses	**11**	**± 1σ**	**8**	**± 1σ**	**8**	**± 1σ**	**5**	**5**	**10**	**± 1σ**	**18**	**± 1σ**	**6**	**± 1σ**	**9**	**± 1σ**	**10**	**± 1σ**	**6**	**± 1σ**	**4**	**5**	**5**	**8**	**± 1σ**	**10**	**± 1σ**	**14**	**± 1σ**	**13**	**± 1σ**	**5**	**18**	**± 1σ**	**10**	**± 1σ**
SiO_2	48.66	2.58	51.63	0.30	50.47	0.84	51.05	52.83	51.67	0.66	51.15	0.41	51.12	0.28	51.94	0.17	52.54	0.35	52.17	0.19	52.71	51.52	54.12	51.52	0.20	51.55	0.15	52.05	0.58	51.63	1.06	51.11	50.91	0.82	51.54	0.20
TiO_2	1.71	0.84	0.69	0.03	1.01	0.24	0.64	0.34	0.51	0.10	0.70	0.11	0.71	0.07	0.69	0.04	0.58	0.04	0.63	0.03	0.47	0.66	0.29	0.67	0.04	0.65	0.05	0.65	0.11	0.77	0.15	0.68	0.71	0.13	0.79	0.06
Al_2O_3	3.98	1.86	1.99	0.15	2.62	0.48	1.98	0.97	1.76	0.42	2.25	0.23	2.20	0.30	1.76	0.16	2.14	0.13	2.00	0.20	2.28	1.57	1.58	2.01	0.14	2.05	0.19	2.16	0.21	2.01	0.74	1.79	2.07	0.34	2.38	0.15
Cr_2O_3	0.02	0.01	0.04	0.02	0.02	0.03	0.01	0.02	0.07	0.09	0.03	0.02	0.15	0.08	0.01	0.02	0.09	0.06	0.00	0.00	0.15	0.00	0.13	0.13	0.03	0.13	0.02	0.02	0.02	0.01	0.01	0.05	0.06	0.08	0.33	0.04
FeO	14.49	1.64	11.89	0.15	13.53	1.02	12.23	19.11	11.19	3.56	10.24	0.50	9.76	0.75	12.35	0.41	11.05	0.39	12.74	0.17	10.37	12.12	14.59	10.63	0.23	10.83	0.33	11.48	0.51	12.53	0.88	12.10	13.23	1.85	8.38	0.17
MnO	0.34	0.02	0.34	0.02	0.36	0.03	0.35	0.54	0.33	0.11	0.32	0.06	0.33	0.08	0.37	0.03	0.32	0.02	0.36	0.01	0.31	0.43	0.39	0.31	0.02	0.32	0.02	0.34	0.02	0.36	0.04	0.34	0.38	0.07	0.25	0.01
MgO	11.48	2.87	14.94	0.10	13.82	0.99	14.79	21.07	14.76	1.81	15.83	0.69	15.99	0.25	14.76	0.23	15.18	0.15	14.94	0.19	16.03	14.38	26.62	15.71	0.19	15.82	0.39	15.00	0.41	14.39	0.99	14.80	13.92	1.07	15.94	0.18
CaO	18.83	0.84	18.22	0.16	17.87	1.20	17.82	4.51	18.97	1.21	18.31	0.53	18.32	0.30	18.06	0.23	18.15	0.16	17.63	0.44	18.43	18.06	1.84	17.87	0.23	17.88	0.28	18.44	0.22	18.08	0.48	18.00	17.81	0.59	19.33	0.26
Na_2O	0.33	0.06	0.25	0.03	0.26	0.03	0.27	0.07	0.25	0.05	0.36	0.05	0.32	0.02	0.27	0.02	0.26	0.02	0.27	0.02	0.27	0.37	0.02	0.25	0.02	0.27	0.03	0.31	0.02	0.27	0.02	0.27	0.36	0.19	0.31	0.01
K_2O	0.01	0.02	0.00	0.00	0.01	0.01	0.00	0.00	0.00	0.00	0.00	0.00	0.00	0.00	0.00	0.00	0.00	0.00	0.00	0.00	0.00	0.00	0.00	0.00	0.00	0.00	0.00	0.00	0.01	0.01	0.01	0.00	0.00	0.00	0.00	0.00
NiO	0.01	0.01	0.01	0.02	0.01	0.01	0.00	0.02	0.02	0.02	0.01	0.02	0.00	0.01	0.01	0.01	0.01	0.01	0.00	0.00	0.00	0.01	0.03	0.02	0.01	0.02	0.01	0.01	0.01	0.01	0.01	0.02	0.02	0.01	0.01	0.01
Total	100.14	0.57	100.05	0.31	100.08	0.27	99.15	99.46	99.52	0.38	99.20	0.42	98.90	0.17	100.29	0.18	100.39	0.39	100.74	0.35	101.02	99.13	99.60	99.12	0.23	99.54	0.33	100.51	0.51	100.14	1.04	99.26	99.52	0.61	99.27	0.23
Mg#	0.60	0.09	0.71	0.01	0.67	0.03	0.71	0.66	0.72	0.10	0.78	0.01	0.78	0.02	0.69	0.01	0.71	0.01	0.69	0.01	0.75	0.69	0.77	0.74	0.01	0.75	0.02	0.72	0.01	0.68	0.03	0.71	0.68	0.05	0.79	0.01
En	34.08	7.15	42.80	0.20	40.06	2.64	42.64	59.63	42.27	4.61	45.29	1.76	45.90	0.72	42.30	0.56	43.87	0.40	42.72	0.50	45.44	41.77	73.24	45.26	0.38	45.26	0.68	42.97	1.03	41.51	2.00	42.59	40.46	2.69	45.96	0.51
Fs	25.22	3.97	19.71	0.28	22.68	1.85	20.43	31.21	18.66	6.15	17.06	0.92	16.32	1.33	20.50	0.66	18.44	0.64	21.05	0.38	17.01	20.52	23.13	17.73	0.39	17.97	0.56	19.05	0.91	20.96	1.89	20.18	22.31	3.33	14.00	0.26
Wo	40.70	3.32	37.50	0.29	37.25	2.52	36.92	9.17	39.07	2.08	37.65	1.21	37.79	0.64	37.20	0.56	37.69	0.37	36.23	0.69	37.55	37.72	3.63	37.01	0.51	36.77	0.69	37.97	0.40	37.53	0.53	37.23	37.23	0.99	40.04	0.53

All samples were altered to some extent, but those taken from massive centers are much fresher than tops and bottoms. Typical alteration features are partial albitization and/or sericitization of the plagioclase, partial or complete replacement of mafic minerals by chlorite, and glass crystallization to titanite and chlorite. Epidote, quartz, calcite, K-feldspar and minor amounts of pumpellyite, prehnite, actinolite and zeolite can be found depending on the alteration degree (Table 1b).

The composition of the plutonic rock varies from diorite to granite (Table 1a). These rocks are much fresher than the volcanic rocks, although in some samples sericite, chlorite, titanite, actinolite, tourmaline and biotite are present as secondary mineral phases. Partial replacement of clinopyroxene by hornblende occurred as a result of the cooling process of these rocks. Sample RS18 from Michilla is a diorite with ortho and clinopyroxene, with rather homogeneous Mg# (0.77 to 0.69, Table 1a, Fig. 2b).

WHOLE-ROCK CHEMISTRY

The major, trace and rare earth (REE) elements abundances for the studied volcanic and plutonic rocks are listed in table 4.

ALTERATION

All the studied rock samples are altered to some extent. Alteration is much stronger in volcanic than in plutonic rocks and in the top and bottom of the lava flows than in the centers. Although samples containing amygdales and veinlets were avoided, no wholly fresh rocks were analyzed. Therefore, in order to observe the mobility of the elements due to the alteration processes, six strongly altered rocks, with high LOI, abundant sericite and chlorite in phenocrysts, abundant calcite, pumpellyite or actinolite and/or oxidation of the groundmass, were sampled and analyzed to be compared with fresher rocks. A probable alkali addition by alteration processes is inferred when comparing the total alkali *versus* silica classification (TAS) diagram with the Zr/TiO_2 *versus* Nb/Y classification diagram for altered rocks. In the first diagram an important number of samples plot in the trachy-andesite, basaltic trachy-andesite and trachy-basalt fields, in the second diagram they only plot in the andesite and basaltic andesite fields (Fig. 3). Therefore, the alkali enrichment of these samples is likely due to the albitization/sercitization of the plagioclase phenocrysts but not to magmatic processes. The altered samples also show a higher dispersion for large ion lithophile elements (LILE) than high field strength elements (HSFE) relative to the fresher samples, suggesting that HFSE are less mobile. The REE show a global enrichment (Iquique, Mantos Blancos, Antofagasta areas) or depletion (Arica, Tocopilla and Michilla areas), but patterns of altered and fresh samples have no significant differences.

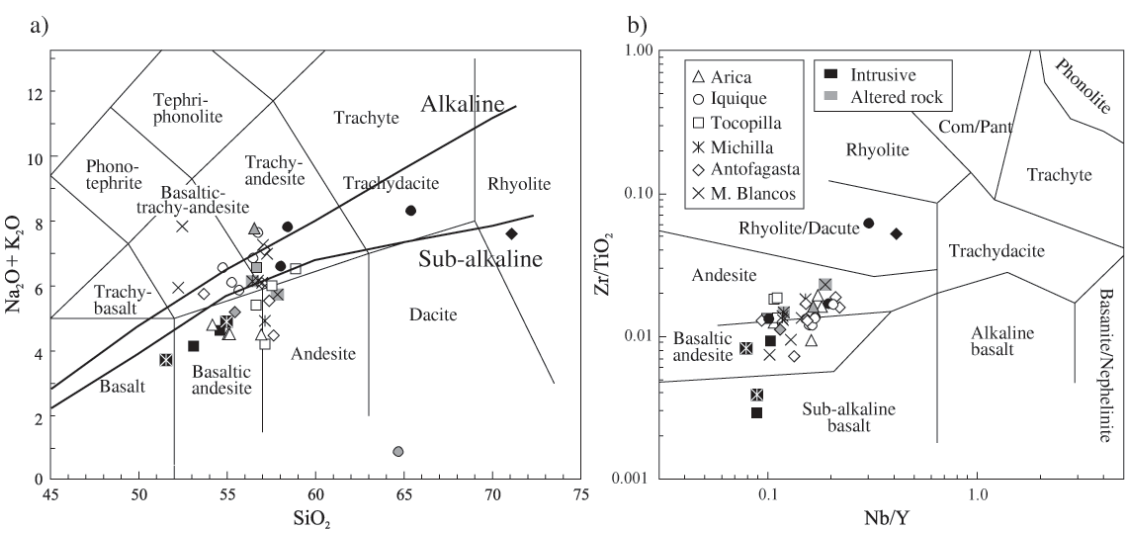

FIG. 3. **a-** Total alkali *versus* silica classification diagram (TAS, Le Maitre *et al.,* 1989); **b-** Zr/TiO_2 *versus* Nb/Y classification diagram for altered volcanic rocks (after Winchester and Floyd, 1977). Alkaline and sub-alkaline limits are after Rickwood (1989).

The most altered sample (VO164) was collected in the Iquique area and corresponds to a highly altered top of a lava flow, where pumpellyite, epidote, quartz, chlorite and K-feldspar have almost completely replaced phenocrysts and groundmass. This sample shows a high dispersion in oxides, except by TiO_2 and P_2O_5, significant depletion in LILE and less important in Sr and Pb, while HSFE and REE contents are relatively similar to the fresh samples. The discussion of the geochemical data will be focused on the HSF and RE elements, which are thought to be immobile during the alteration.

MAJOR ELEMENTS

SiO_2 content (anhydrous base) in the volcanic rocks varies between 50.9% and 57.6%, except VO164 that has a silica content of 63.4% (Fig. 4). The total alkali content varies between 4.1 and 7.6% and in the diagram K_2O *versus* SiO_2 (not shown), the lavas plot mainly on the high-K calc-alkaline series. Nevertheless, as explained above, the high K_2O content of the lavas, also recognized by Palacios (1978) and Buchelt and Tellez (1988) as a distinguishing feature of these rocks, could be due to potassium enrichment during alteration processes.

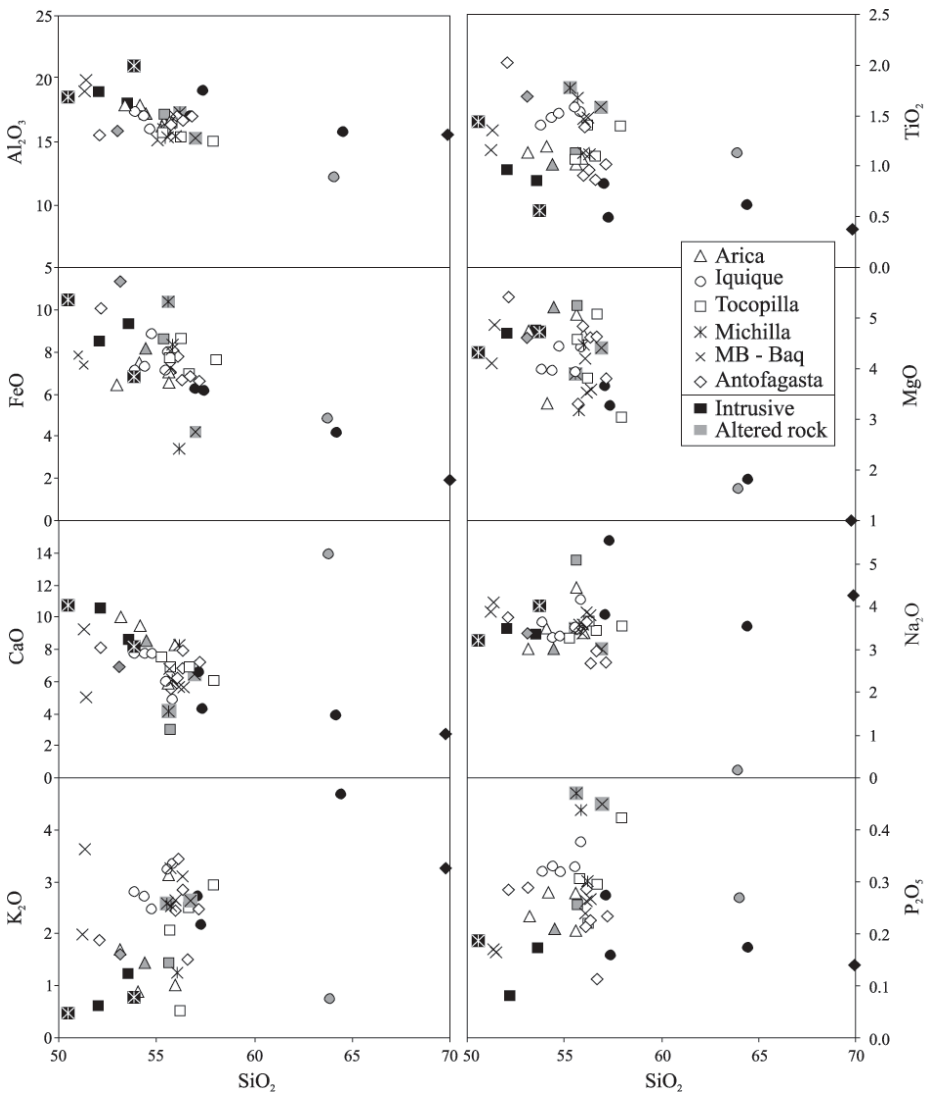

FIG. 4. Major element variations with respect to SiO_2 content (anhydrous base) for the studied samples. Symbols in black represent plutonic rocks and symbols in gray represent altered rocks.

MgO content is low (3.0-5.4%) and Al_2O_3 is high (19.7-14.9%). The variations of major elements with respect to the SiO_2 content are plotted in figure 4. In spite of the small range in the silica content some correlations are observed as the decreasing MgO, CaO, Al_2O_3 and FeO and increasing of K_2O abundances with increasing SiO_2 content, *i.e.,* increasing differentiation. No systematic differences in major elements abundances are observed neither in lavas from different areas nor in rocks with different ages.

Intrusives and a dike show a wider range of SiO_2 content, 50.1 to 69.2%, and better defined trends with decreasing Al_2O_3, FeO, MgO, TiO_2, CaO, increasing K_2O and Na_2O and rather homogeneous P_2O_5. According to their total alkali content they are equivalent to basalt, basaltic andesite, trachy-andesite, trachydacite and rhyolite (Fig. 3). The K_2O *versus* SiO_2 contents for intrusive rocks from Tocopilla, Michilla and Antofagasta area indicate they belong to the calc-alkaline series whereas those from Iquique belong to the high-K calc-alkaline series.

TRACE ELEMENTS AND REE

Multielement patterns for all the studied samples are similar showing a stronger enrichment in LILE than in HFSE with respect to the primitive mantle and variable LILE contents (Fig. 5), since these elements are more mobile during alteration and incompatible during early stages of crystal fractionation. Negative Nb (Nb-Ta trough) and Ti anomalies, and highly variable but rather flat Th-U paths are also common features in the studied rocks. Volcanic rocks from different areas and ages show no significant differences in their trace element patterns except a generally lower LILE enrichment in the lavas from

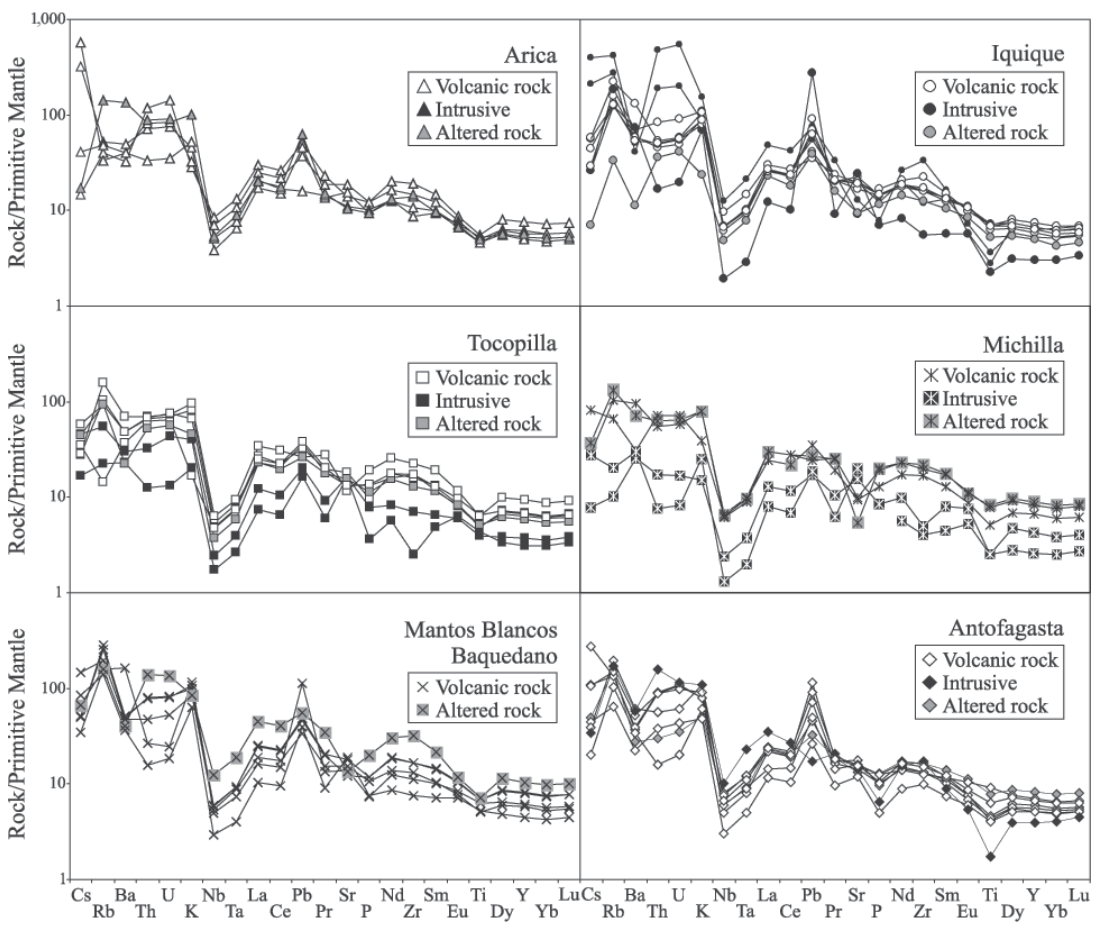

FIG. 5. Primitive mantle-normalized trace element patterns for volcanic and plutonic rocks from the six studied areas in the Coastal Cordillera of northern Chile. Normalizing values are from Sun and McDonough (1989).

the Arica area. Trace element contents in basic plutonic rocks are lower than in the volcanic rocks but the trace element patterns of both are sub-parallel, with steeper Nb and Ti anomalies in the plutonic rocks. In spite of the general large scatter in LILE abundances some systematic patterns are observed: Sr < Ba < Rb and Ba generally lower than Th. Ta, Nb, Zr have a well defined positive correlation with SiO_2 content, whereas Th has also positive correlation but with higher dispersion. Compatible elements such as Cr, Ni and V have negative correlation with SiO_2 (Table 4), Sr behavior seem coupled with Ca as it has also a negative correlation with SiO_2 (Table 4). Cu content does not show correlation either with SiO_2 nor with Mg#, and it is noteworthy to point out that the most altered samples, *e.g.,* VO144, VO177, VO47, VO187, VO164, normally show lower Cu contents than fresher samples (10-70 ppm *versus* 50-200 ppm).

Rare earth elements (REE) (Fig. 6) display fractionated patterns in the volcanic rocks with a higher enrichment in light REE (LREE, La to Sm) than heavy REE (HREE, Gd to Lu) relative to chondrite abundances. $(La/Yb)_N$ ratios range between 2.2 and 5.0. The HREE show a rather flat pattern and have abundances 13-37 times chondritic values, whereas the LREE are 30-80 times the chondritic values. Eu negative anomalies are observed in most of the analyzed lava flows in the volcanic rocks. Some samples from Antofagasta, Mantos Blancos and Iquique areas show slight or no Eu anomaly; they would correspond to the less differentiated rocks because they also have a low Zr content (Zr being an indicator of the differentiation degree) and Eu_N has a clear negative correlation with Zr content. Yb_N and $(La/Lu)_N$ ratios have slight

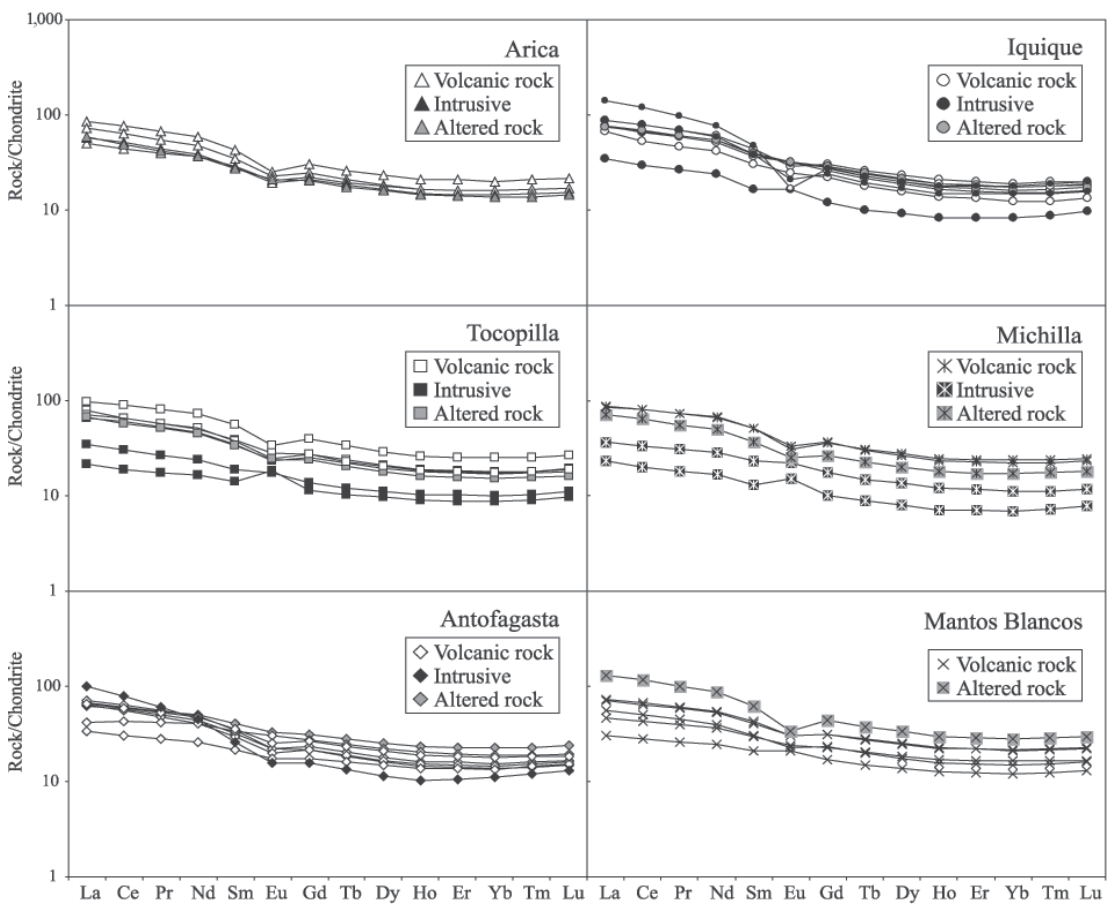

FIG. 6. Chondrite-normalized Rare Earth elements (REE) patterns for volcanic and plutonic rocks from the six studied areas in the Coastal Cordillera of northern Chile. Normalizing values are from Sun and McDonough (1989).

TABLE 4. GEOCHEMICAL ANALYSES OF THE COASTAL CORDILLERA (18°30'-24°S) VOLCANIC AND PLUTONIC ROCKS.

Sample	VO69	VO76	VO175	VO177	VO180	VO50	VO160	VO161	VO163	VO164	VO169	VO170	VO184	VO185	VO2	VO3	VO4	VO150	VO155A	VO156
Type	Lava	Lava	Lava	Lava	Lava	Lava	Lava	Dike	Lava	Lava (A)	Lava	Lava	Intrusive	Intrusive	Lava	Intrusive	Lava	Lava	Lava (A)	Lava
Locality	Arica	Arica	Arica	Arica	Arica	Iquique	Iquique	Iquique	Iquique	Iquique	Iquique	Iquique	Iquique	Iquique	Tocop.	Tocop.	Tocop.	Tocop.	Tocop.	Tocop.
SiO_2 %	51.79	54.04	53.13	54.20	50.26	54.67	52.25	55.34	53.30	60.50	54.24	53.63	55.26	63.06	55.39	52.70	53.22	56.37	53.13	54.22
Al_2O_3 %	17.19	16.06	16.86	15.92	16.90	16.18	16.84	18.32	16.69	11.45	15.52	15.56	16.53	15.38	15.08	17.78	15.66	14.64	16.41	15.38
Fe_2O_3 %	2.82	2.66	1.98	2.53	4.73	2.73	2.73	2.35	2.83	3.59	2.06	1.98	2.47	2.14	2.69	1.50	3.23	2.94	6.41	2.98
FeO %	5.92	5.59	7.13	5.32	2.84	5.73	5.73	4.94	5.94	2.15	7.43	7.13	5.18	2.88	5.64	7.64	6.77	6.17	3.84	6.25
MnO %	0.12	0.13	0.23	0.28	0.17	0.18	0.20	0.20	0.19	0.08	0.22	0.16	0.16	0.10	0.17	0.13	0.20	0.26	0.31	0.16
MgO %	3.18	4.53	5.10	4.93	4.46	4.36	3.89	3.15	3.88	1.54	3.86	4.35	3.54	1.78	4.98	4.67	3.60	2.97	5.01	4.47
CaO %	9.05	8.00	8.31	5.71	9.46	4.85	7.48	4.19	7.57	13.16	5.80	7.60	6.34	3.77	6.72	8.46	6.54	5.88	2.87	7.36
Na_2O %	3.32	3.22	2.90	4.32	2.82	4.04	3.50	5.30	3.19	0.11	3.39	3.21	3.65	3.42	3.34	3.27	3.42	3.41	4.81	3.18
K_2O %	0.86	0.99	1.40	3.06	1.58	3.28	2.72	2.09	2.66	0.72	3.16	2.42	2.62	4.58	2.44	1.20	0.50	2.85	1.37	2.01
TiO_2 %	1.15	1.04	0.99	0.99	1.08	1.51	1.35	0.48	1.45	1.07	1.55	1.49	0.79	0.60	1.06	0.84	1.33	1.35	1.08	1.04
P_2O_5 %	0.27	0.27	0.21	0.20	0.22	0.37	0.31	0.15	0.33	0.26	0.32	0.31	0.27	0.17	0.29	0.17	0.21	0.41	0.25	0.30
LOI %	3.98	2.70	2.20	2.14	6.15	1.34	2.24	2.39	1.58	4.58	2.06	1.56	1.54	0.70	1.48	0.65	4.06	2.01	3.93	1.67
Total %	99.65	99.24	100.45	99.61	100.66	99.24	99.26	98.91	99.61	99.20	99.62	99.41	98.34	98.58	99.27	99.01	98.74	99.29	99.41	99.00
Mg#	0.49	0.59	0.58	0.62	0.74	0.58	0.55	0.53	0.54	0.56	0.51	0.52	0.55	0.52	0.61	0.52	0.49	0.46	0.70	0.56
Ba ppm	227	278	346	953	280	488	417	513	374	80	908	400	286	359	335	211	257	491	159	335
Rb ppm	26	21	33	90	31	118	102	78	81	21	141	79	173	266	67	35	9	101	60	59
Th ppm	10.0	7.5	6.1	6.9	2.8	7.1	3.8	1.4	4.3	3.1	4.5	4.2	16.0	40.4	5.7	2.8	5.3	6.0	4.4	5.8
Nb ppm	6.0	5.0	2.8	3.9	3.6	6.9	4.4	1.4	4.8	3.5	4.9	4.8	4.7	8.9	3.9	1.7	3.5	4.5	2.6	3.3
Sr ppm	295	393	324	219	235	196	474	517	402	196	422	356	419	272	277	349	384	245	327	282
Zr ppm	217	163	121	158	97	252	180	63	193	140	185	181	133	372	193	78	180	249	144	195
Y ppm	35	28	26	24	23	34	27	14	29	23	30	30	24	29	29	17	31	42	27	30
Cr ppm	33	59	56	54	57	78	23	5	25	19	7	54	8	< D.L.	157	139	20	24	33	69
V ppm	218	236	255	197	259	225	268	116	283	210	338	301	180	96	213	282	330	189	320	246
Ni ppm	18	27	20	29	20	32	19	< D.L.	19	9	16	23	8	< D.L.	38	24	18	13	16	22
Co ppm	25	26	27	26	23	24	25	17	27	12	25	27	19	11	24	26	27	21	27	29
Cs ppm	0.5	18.2	10.4	0.5	1.3	0.8	0.9	0.8	1.8	0.2	1.8	1.4	6.7	12.8	0.9	1.5	1.1	0.9	1.4	1.9
Pb ppm	9.3	6.8	8.5	11.6	2.9	6.5	7.6	51.3	11.5	7.3	16.9	12.9	10.1	13.9	6.6	3.7	5.9	4.9	4.9	7.0
Cu ppm	168	147	468	7	7	156	15	21	38	5	45	7	228	136	137	20	290	348	18	53
Zn ppm	92	81	87	152	85	136	135	184	114	51	173	100	133	372	179	44	110	136	186	98
Ta ppm	0.55	0.44	0.27	0.37	0.32	0.61	0.39	0.12	0.41	0.32	0.42	0.41	0.43	0.87	0.35	0.16	0.31	0.38	0.24	0.30
Hf ppm	5.7	4.3	3.5	4.1	2.8	5.9	4.5	1.8	4.9	3.5	4.8	4.7	4.3	10.5	4.8	2.2	4.6	6.5	4.1	5.2
U ppm	3.0	1.9	1.6	1.8	0.7	1.9	1.0	0.4	1.2	0.9	1.2	1.1	4.2	11.3	1.5	0.9	1.4	1.5	1.2	1.6
La ppm	20	17	12	14	14	21	18	8	18	16	18	18	21	33	16	8	19	23	16	17
Ce ppm	47	39	27	31	30	48	40	18	42	32	41	41	48	74	37	18	40	54	35	40
Pr ppm	6.4	5.2	3.8	4.2	4.0	6.6	5.5	2.5	5.8	4.4	5.7	5.7	6.5	9.3	5.0	2.5	5.4	7.7	4.9	5.5
Nd ppm	28	22	17	18	17	28	24	11	25	19	25	25	27	36	22	11	24	34	21	24
Sm ppm	6.6	5.4	4.4	4.3	4.1	6.7	5.6	2.6	5.9	4.6	6.1	6.1	5.9	7.2	5.3	2.9	5.8	8.5	5.1	5.8
Eu ppm	1.4	1.3	1.2	1.1	1.2	1.7	1.8	1.0	1.8	1.4	1.8	1.9	1.2	1.0	1.3	1.0	1.6	2.0	1.4	1.4
Gd ppm	6.3	5.1	4.5	4.4	4.2	6.3	5.4	2.5	5.7	4.6	5.9	5.9	4.9	5.7	5.2	2.8	5.6	8.1	4.9	5.6
Tb ppm	0.98	0.78	0.73	0.69	0.65	0.98	0.80	0.38	0.86	0.67	0.90	0.92	0.72	0.85	0.82	0.45	0.89	1.26	0.76	0.85
Dy ppm	5.9	4.7	4.6	4.2	4.0	5.8	4.7	2.3	5.1	4.0	5.4	5.5	4.3	5.1	5.0	2.8	5.3	7.4	4.6	5.2
Ho ppm	1.2	0.9	0.9	0.8	0.8	1.2	0.9	0.5	1.0	0.8	1.1	1.1	0.8	1.0	1.0	0.6	1.1	1.5	0.9	1.0
Er ppm	3.4	2.7	2.7	2.4	2.4	3.3	2.6	1.4	2.8	2.2	3.0	3.1	2.4	3.0	2.9	1.7	3.1	4.2	2.6	3.0
Yb ppm	3.5	2.8	2.8	2.5	2.3	3.3	2.6	1.5	2.8	2.1	3.0	3.0	2.5	3.2	2.9	1.8	3.1	4.3	2.7	3.0
Tm ppm	0.51	0.41	0.41	0.37	0.35	0.49	0.39	0.21	0.42	0.32	0.45	0.45	0.38	0.46	0.44	0.26	0.46	0.65	0.39	0.45
Lu ppm	0.54	0.43	0.43	0.39	0.37	0.51	0.41	0.25	0.44	0.34	0.47	0.48	0.40	0.50	0.46	0.28	0.50	0.67	0.41	0.48

Tocop.: Tocopilla; **MB&B:** Mantos Blancos and Baquedano; **Antof.:** Antofagasta; **<D.L.:** below detection level; **Mg#:** Mg/(Fe+Mg).

Table 4 (continuation)

Sample	VO183	VO144	VO147	VO148	VO181	RS18	VO13	VO130B	VO131B	VO187	VO191	VO193	VO36A	VO37	VO40B	VO48	VO47	VO137	VO142	VO136
Type	Intrusive	Lava	Lava	Lava	Intrusive	Intrusive	Lava (M)	Lava	Lava	Lava (A)	Lava	Lava	Lava	Lava	Lava	Lava	Lava (A)	Lava	Lava	Intrusive
Locality	Tocop.	Michilla	Michilla	Michilla	Michilla	Michilla	MB & B	MB & B	MB & B	MB & B	MB & B	MB & B	Antof.	Antof.	Antof.	Antof.	Antof.	Antof.	Antof.	Antof.
SiO_2 %	51.08	51.92	51.97	52.99	49.95	52.52	49.93	54.64	54.54	55.26	54.31	49.70	54.35	55.71	54.74	55.21	51.43	50.75	54.06	69.96
Al_2O_3 %	18.57	14.27	15.94	15.28	18.28	20.48	19.31	15.42	15.09	14.76	16.10	18.41	16.67	16.71	16.65	16.32	15.37	15.12	15.87	15.61
Fe_2O_3 %	1.36	3.84	4.33	3.14	1.68	1.09	1.98	3.08	3.11	5.56	2.76	2.83	2.68	2.54	2.56	2.65	1.98	1.98	2.98	0.58
FeO %	6.93	8.06	2.60	6.60	8.59	5.56	7.13	6.46	6.54	3.34	5.79	5.94	5.62	5.34	5.37	5.56	7.13	7.13	6.26	2.07
MnO %	0.14	0.11	0.12	0.39	0.19	0.15	0.21	0.24	0.24	0.16	0.19	0.18	0.12	0.20	0.26	0.16	0.52	0.22	0.20	0.05
MgO %	4.61	3.65	4.15	3.02	4.28	4.61	4.72	3.45	3.47	4.27	4.07	3.98	4.68	3.72	4.48	4.52	4.47	5.27	3.22	1.01
CaO %	10.34	3.83	7.64	5.73	10.58	7.98	4.89	5.44	5.47	6.21	6.58	8.96	6.02	7.00	6.63	7.74	6.61	7.85	5.37	2.69
Na_2O %	3.38	3.23	3.32	3.37	3.15	3.92	3.95	3.74	3.64	2.90	3.26	3.73	3.40	2.59	2.58	2.84	3.25	3.60	3.48	4.23
K_2O %	0.62	2.42	1.17	2.39	0.45	0.77	3.50	3.21	3.01	2.58	2.54	1.92	2.37	2.42	2.75	1.46	1.54	1.82	3.29	3.26
TiO_2 %	0.95	1.68	1.04	1.61	1.43	0.54	1.32	1.44	1.44	1.54	1.10	1.13	0.88	0.99	0.93	0.85	1.64	1.97	1.33	0.38
P_2O_5 %	0.08	0.44	0.28	0.42	0.19		0.16	0.26	0.26	0.44	0.23	0.17	0.21	0.23	0.22	0.11	0.28	0.28	0.28	0.14
LOI %	0.42	5.45	6.87	5.17	0.79	1.57	2.04	1.70	1.70	2.06	2.26	2.59	2.22	1.76	2.12	1.33	2.22	1.91	1.98	0.69
Total %	98.48	98.90	99.42	100.11	99.54	99.19	99.15	99.07	98.50	99.08	99.18	99.53	99.22	99.21	99.28	98.74	96.45	97.90	98.30	100.68
Mg#	0.54	0.45	0.74	0.45	0.47	0.60	0.54	0.49	0.49	0.70	0.56	0.54	0.60	0.55	0.60	0.59	0.47	0.53	0.48	0.54
Ba ppm	162	502	213	674	178	210	1134	361	339	285	334	257	256	271	363	158	196	236	423	409
Rb ppm	14	84	42	65	6	13	102	179	163	102	123	89	86	85	94	41	97	65	125	109
Th ppm	1.1	5.3	6.1	4.7	1.5	0.6	2.3	6.7	6.8	11.7	4.1	1.3	7.5	7.8	7.5	3.2	2.5	1.3	4.7	13.5
Nb ppm	1.2	4.7	4.5	4.4	1.7	0.9	3.6	4.2	4.2	8.8	3.8	2.1	3.5	5.7	5.5	2.1	4.3	4.3	4.7	7.2
Sr ppm	345	113	199	210	323	427	289	256	378	282	321	402	375	335	302	251	283	332	330	301
Zr ppm	28	242	186	219	56	45	125	185	188	355	148	84	150	183	149	110	185	142	171	195
Y ppm	14	40	30	38	19	12	28	36	37	47	26	21	23	27	25	23	38	32	31	18
Cr ppm	74	6	68	15	40	36	82	39	41	79	46	45	39	41	51	88	36	91	21	6
V ppm	330	315	195	308	532	151	259	288	296	177	247	304	205	201	201	230	368	337	276	34
Ni ppm	32	9	31	12	29	48	43	21	23	31	26	28	20	20	28	40	21	36	15	< D.L.
Co ppm	27	25	31	22	32	28	31	26	28	22	26	28	24	23	22	28	31	30	26	4
Cs ppm	0.5	1.2	2.6	0.9	0.2	0.9	1.1	1.6	1.6	2.1	4.7	2.7	8.8	3.5	3.4	1.4	1.6	0.6	1.2	1.1
Pb ppm	3.1	5.0	6.6	4.5	3.2	3.5	20.9	8.6	9.1	10.3	6.2	7.4	8.5	16.8	13.1	4.8	6.0	9.1	21.2	3.2
Cu ppm	25	4	15	87	56	69	< D.L.	79	83	63	21	31	88	104	116	209	68	131	40	5
Zn ppm	28	98	83	757	56	99	218	271	785	355	148	84	78	181	156	102	300	118	287	17
Ta ppm	0.11	0.41	0.40	0.37	0.15	0.08	0.31	0.38	0.39	0.78	0.36	0.17	0.33	0.49	0.50	0.21	0.37	0.37	0.45	0.94
Hf ppm	1.0	6.2	4.8	5.6	1.7	1.2	3.3	5.3	5.4	9.3	4.1	2.3	4.0	4.7	3.9	2.9	4.8	3.7	4.7	5.3
U ppm	0.3	1.4	1.5	1.2	0.4	0.2	0.5	1.7	1.7	2.8	1.1	0.4	2.3	2.3	2.1	0.9	0.7	0.4	1.3	2.4
La ppm	5	20	17	21	9	6	11	17	17	31	13	7	15	17	15	16	8	10	16	24
Ce ppm	11	49	39	50	20	12	26	39	41	71	31	17	35	39	34	37	19	26	36	48
Pr ppm	1.6	6.9	5.3	7.0	2.9	1.7	3.7	5.6	5.7	9.6	4.3	2.5	4.7	5.3	4.5	5.2	2.7	4.0	5.1	5.7
Nd ppm	8	31	24	31	13	8	17	25	26	41	19	12	21	23	19	24	12	19	22	21
Sm ppm	2.2	7.8	5.7	7.7	3.6	2.0	4.5	6.3	6.5	9.5	4.6	3.2	4.9	5.3	4.6	6.2	3.3	5.2	5.5	4.0
Eu ppm	1.1	1.8	1.5	1.9	1.3	0.9	1.4	1.7	1.8	2.0	1.3	1.2	1.3	1.3	1.2	1.9	1.0	1.7	1.5	0.9
Gd ppm	2.4	7.5	5.5	7.5	3.6	2.1	4.6	6.4	6.4	9.1	4.8	3.5	4.4	4.9	4.4	6.4	3.6	5.6	5.5	3.2
Tb ppm	0.38	1.16	0.86	1.13	0.56	0.33	0.76	1.02	1.05	1.40	0.74	0.56	0.68	0.76	0.70	1.04	0.60	0.91	0.88	0.50
Dy ppm	2.5	7.0	5.1	6.7	3.5	2.0	4.7	6.2	6.4	8.6	4.5	3.5	4.1	4.6	4.3	6.4	3.8	5.6	5.3	2.9
Ho ppm	0.5	1.4	1.0	1.3	0.7	0.4	1.0	1.3	1.3	1.7	0.9	0.7	0.8	0.9	0.9	1.3	0.8	1.1	1.1	0.6
Er ppm	1.5	4.0	2.9	3.8	1.9	1.2	2.8	3.6	3.7	4.8	2.5	2.1	2.3	2.6	2.4	3.8	2.3	3.2	3.0	1.7
Yb ppm	1.5	4.1	3.0	3.8	1.9	1.2	2.8	3.6	3.7	4.8	2.6	2.1	2.4	2.7	2.6	3.8	2.4	3.2	3.1	2.0
Tm ppm	0.22	0.61	0.44	0.57	0.29	0.18	0.42	0.54	0.54	0.72	0.38	0.31	0.35	0.39	0.37	0.58	0.34	0.48	0.46	0.28
Lu ppm	0.25	0.62	0.45	0.59	0.30	0.20	0.43	0.57	0.57	0.75	0.41	0.33	0.38	0.43	0.41	0.60	0.38	0.49	0.47	0.33

positive correlations with SiO_2 and Zr, though the scatter of the Si_2O content is large. Basic plutonic rocks from Tocopilla and Michilla areas show less enriched trace element patterns, positive Eu anomalies and less fractionated LREE/HREE than volcanic rocks. Nevertheless, three samples from Mantos Blancos-Baquedano area, with low (49%) to normal (54%) SiO_2 content, show a similar pattern (Fig. 6). Positive Eu anomalies characterize also these rocks. The opposite is observed in the granitic intrusives (VO184 in Iquique area and VO153 in Antofagasta area) for which LREE are strongly enriched, whereas the HREE maintain the flat pattern.

The dike from the Iquique area (sample VO161) shows a distinctive pattern relative to the contemporaneous plutons (VO184 and VO185) and to the Oficina Viz lavas. It is slightly less enriched in LILE and has significant lower content in HFSE, very pronounced Th, Nb and TiO_2 negative anomalies and a Pb positive anomaly. It has a very flat REE pattern, as much as the basic intrusives in Tocopilla and Michilla, and an Eu positive anomaly.

DISCUSSION

A remarkable feature of the studied volcanic samples, and in general of the volcanic rocks from the Coastal Cordillera of northern Chile, is their textural, mineralogical and chemical homogeneity, as pointed out by Lucassen *et al.* (2006) and supported by this work. Porphyritic intermediate lavas are by far the more abundant rocks and their geochemical characteristics are shared by rocks of extreme areas (Arica-Antofagasta, 700 km apart) and ages (Iquique, Tocopilla and Antofagasta areas, 175-170, 165-160 and 150-154 Ma, respectively). The general higher enrichment in LILE than HFSE, LREE/HREE fractionation, Nb-Ta trough and the enrichment of Pb relatively to Ce are common features in all studied samples; such characteristics are considered as representative of a subduction-related origin for the magmas (Pearce, 1982). Nevertheless, some differences are observed in the trace element abundances between plutonic and volcanic rocks, as well as in volcanic rocks with low SiO_2 content. These differences are mainly represented by subparallel but more or less enriched trace element patterns, depending on whether the rocks are more or less differentiated relatively to the main group of volcanic rocks. These chemical variations indicate therefore that the rocks from the Coastal Cordillera were likely to have evolved and differentiated mainly by fractional crystallization. The Pearce ratio diagrams show that crystal fractionation was dominated by the crystallization of plagioclase and olivine and, probably, clinopyroxene to a lesser extent (Fig. 7).

CONSTRAINTS ON MAGMA SOURCES AND EVOLUTION

Despite the quantity of data, the Mg# (45-74) and the MgO% (1.01-5.27) of the analyzed rocks (Table 4) indicate that no primitive magmas were analyzed and suggest previous olivine fractionation. Sr isotopic signatures for the volcanic rocks from the Iquique, Arica, Tocopilla and south of Antofagasta areas indicate that the magmas were derived from a depleted mantle source (Rogers and Hawkesworth, 1989; Lucassen and Franz, 1994; Kramer *et al.*, 2005). Zr/Nb ratios are indicative of mantle depletion as they are not influenced by fluid enrichment or fractional crystallization; Nb/Zr ratios from the studied samples have a narrow range similar to the normal mid-ocean ridge basalts (N-MORB) composition and indicate either slight depletion or enrichment relative to N-MORB (Fig. 8a). These ratios do not show a significant variation with time. Low chondritic normalized $(La/Yb)_N$ ratios (2.2-5.0) or flat REE patterns are interpreted as the result of high degrees of partial melting from a mantelic source. Yb_N>10 excludes the possibility of the garnet as a residual phase in the source of the magmas.

The poor radiogenic Sr signatures for the Jurassic volcanic and plutonic rocks would rule out crustal contamination as a major factor in differentiation and evolution of the parental magmas; nevertheless, Pb signatures in lavas from the Iquique area indicate that the Pb system is dominated by crustal signature

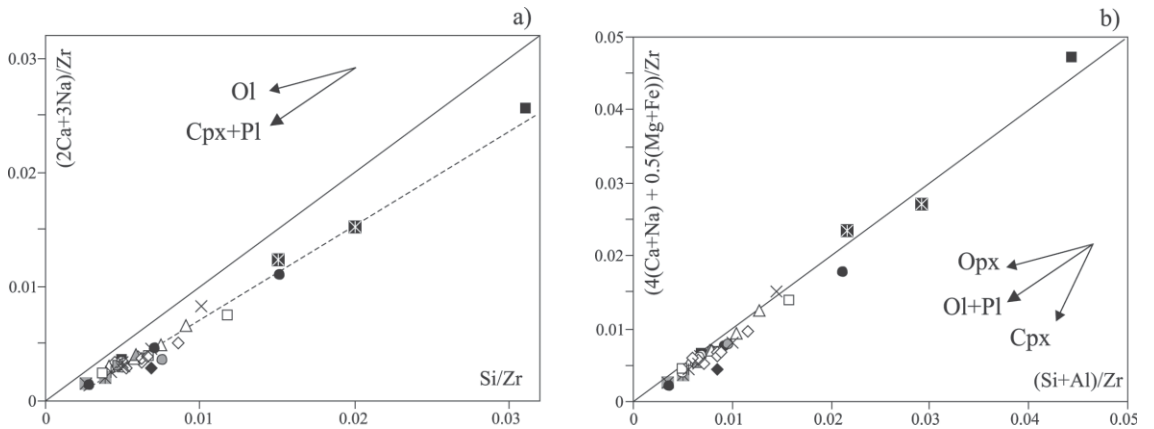

FIG. 7. The Pearce ratio diagrams (Russell and Nichols, 1988) applied to volcanic and plutonic rocks from the Coastal Cordillera of northern Chile in order to test the hypothesis of fractional crystallization dominated by a) plagioclase and clinopyroxene (cpx+pl) or b) plagioclase and olivine (ol+pl). Vectors for orthopyroxene are also plotted (opx). Symbols are as in figure 6.

(Kramer *et al.*, 2005). In the Th/Yb *versus* Ta/Yb diagram, the studied samples follow either the subduction component or the crustal contamination trends (Fig. 9).

The Ba, K and Sr abundances relative to HFSE elements such as Nb and Ta would favour the hypothesis of fluid enrichment in the slab/mantle boundary (Peate *et al.*, 1997). Addition of slab melts into the mantle wedge has been invoked as a process in the generation of the Oficina Viz Formation lavas in Iquique area (Kramer *et al.*, 2005). In the case of the samples studied here, Nb/Ta ratios are generally lower than the MORB values and Sr/Y ratios are relatively low (<30) (Fig. 8b), therefore a slab melt component is unlikely in the genesis of these rocks.

Th/La and Sm/La ratios can be used to trace sediment addition to the mantle wedge (Plank, 2005); in figure 8c, samples plot directly along the sediment component vector, suggesting that this process was involved in the generation of the parental magmas. In addition, the Th/La ratios for volcanic rocks exhibit a slight positive correlation with age (Fig. 8d), whereas the lavas from Antofagasta, Arica and Tocopilla areas have in general higher Th/La ratios than those from Iquique area. In the Ce/Pb *versus* Nb/U diagram the samples plot in the arcs field but also in the marine sediments field (Fig. 8e).

Ba/Ta and Ce/Pb ratios show no correlation when plotted *versus* age of the rocks (Fig. 8f,g). The same is valid for major elements, only Ti presents a slight negative correlation, and other trace element ratios such as $(La/Lu)_N$, Nb/Ta, Zr/Y, $(La/Yb)_N$ and Sr/Y. Therefore, the sources that originated the parental magmas and the processes which dominated their evolution and differentiation did not change significantly from 175-170 (Oficina Viz, Iquique area) to 150 Ma (La Negra Formation, Antofagasta). Only the amount of the sediment component added to the mantle wedge during slab/mantle interaction in the subduction zone seems to have increased as the arc evolved. In this sense, and based on Nd, Pb and Sr isotope composition, Lucassen *et al.* (2006) also postulated a rather uniform depleted subarc mantle source over the entire studied region.

TECTONIC SETTING FOR THE VOLCANIC AND PLUTONIC ROCKS

The projection of the chemical features of the studied samples on different geotectonic discrimination diagrams confirms the dominant calc-alkaline orogenic signature of these rocks. In the La/10-Y/5-Nb/8 discrimination diagram (Fig. 10), the volcanic rocks cluster near the calc-alkaline/volcanic arc tholeiites transition zone. The compositions of the clinopyroxene phenocrysts show the same pattern (Fig. 2.c) and in the Th/Yb *versus* Ta/Yb diagram (Fig. 9) the volcanic rocks plot near the boundary between the oceanic arc and active continental margin fields of Pearce (1983) or in the active continental margin field of

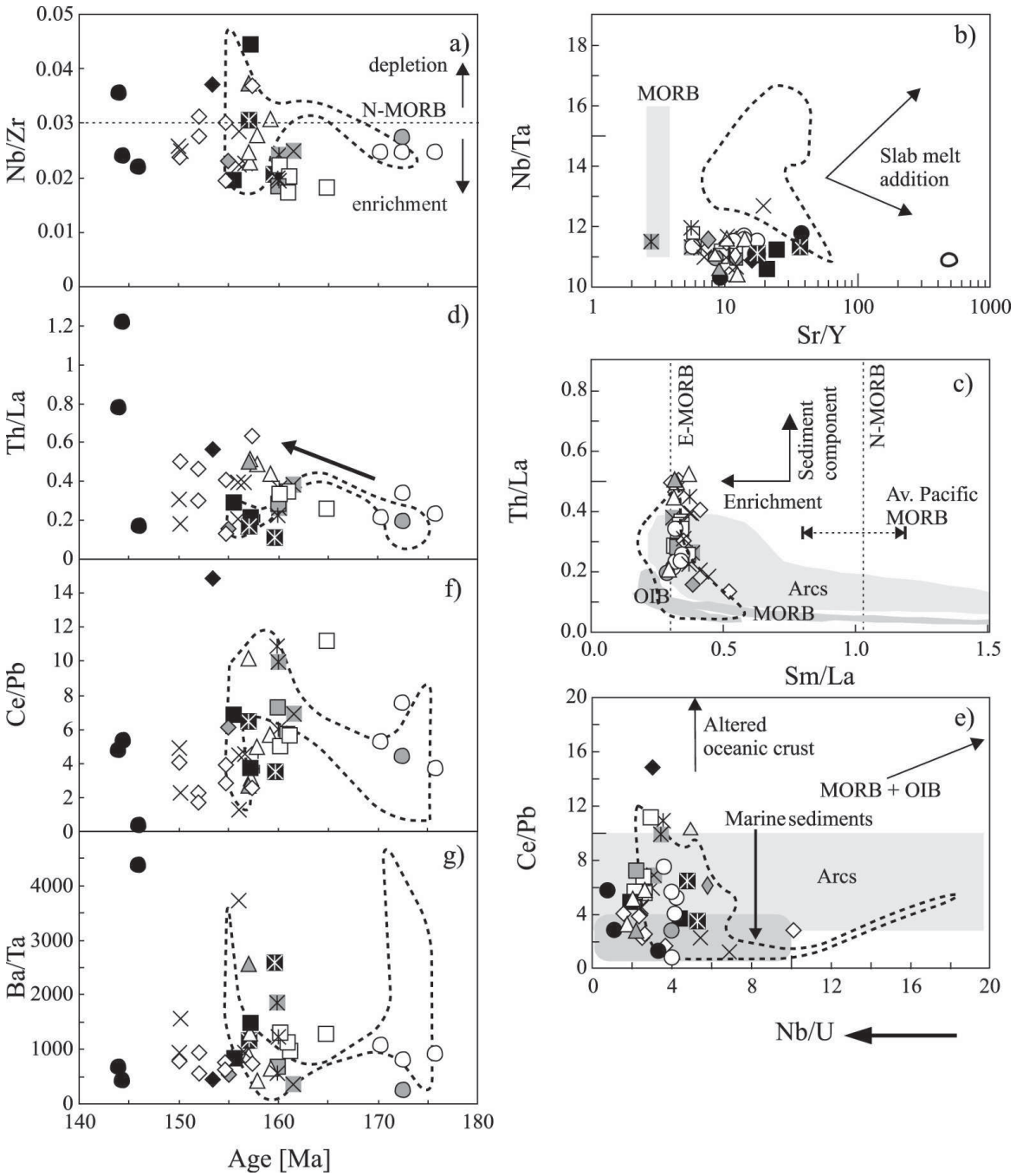

FIG. 8. Plots of: **a-** Nb/Zr *versus* age; **b-** Sr/Y *versus* Nb/Ta; **c-** Sm/La *versus* Th/La; **d-** Th/La *versus* age; **e-** Nb/U *versus* Ce/Pb; **f-** Ba/Ta *versus* age and **g-** Ce/Pb *versus* s age, for volcanic and plutonic rocks from the Coastal Cordillera of northern Chile. In a), N-MORB Nb/Zr average value (dotted line) is from Sun and McDonough (1989); b), MORB field Sr/Y values are from Hoffmann (1988) and Na/Ta values from Münker *et al.* (2003) and Büchl *et al.* (2002), vectors from Münker *et al.* (2003); in c), arcs, OIB and MORB fields, enrichment and sediments component vectors and average Sm/La values for normal, enriched and Pacific MORB (dotted lines: N-MORB, E–MORB, Pacific) are as used by Plank (2005); in e), marine sediments and arcs fields as wells as altered oceanic crust and OIB+MORB vectors are after Klein and Karsten (1995). See table 1 for ages. Symbols are as in figure 4. Areas inside dotted lines represent data from Kramer *et al.* (2005), the ages were estimated by those authors based on stratigraphic relations and fossil record.

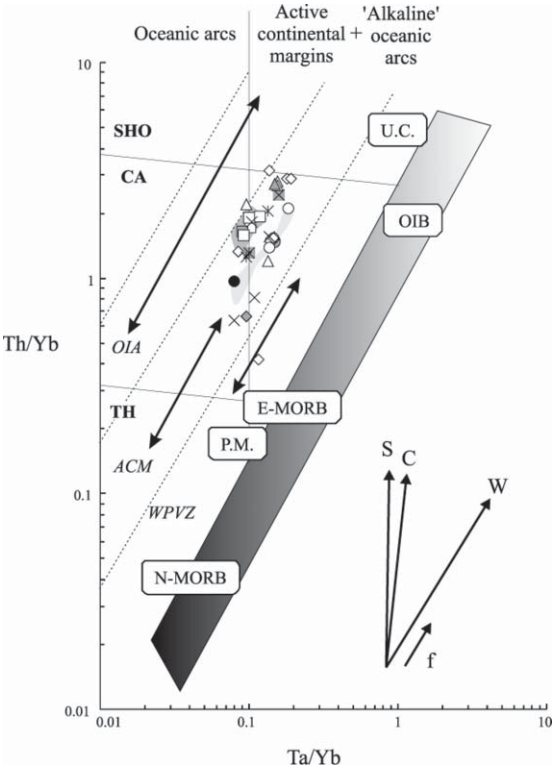

FIG. 9. Ta/Yb *versus* Th/Yb diagram (Pearce 1982, 1983) for the volcanic rocks and a dike from the Coastal Cordillera of northern Chile. Shaded areas represent intermediate Jurassic volcanic rock data from Tocopilla (**dark gray**; La Negra Formation, Rogers, 1985) and Iquique areas **(light gray**, Oficina Viz Formation, Kramer *et al.*, 2005). **C**, crustal contamination vector; **W**, within-plate enrichment vector; **S**, subduction zone enrichment vector; **f,** fractional crystallization vector; **SHO**, shoshonitic series; **CA**, calc-alkaline series; **TH**, tholeiitic series. Mid-ocean ridge and within-plate volcanic rocks plot along the diagonal shaded band. The vertical boundary between oceanic arc and active continental margins (Ta/Yb = 0.1) from Pearce (1983). Diagonal dotted lines divide the fields of oceanic arcs **(OA)**, active continental margins **(ACM**), and within-plate volcanic zones **(WPVZ)** (Gorton and Schandl, 2000). **UC**, average composition of the upper continental crust (Wedepohl, 1995). Primitive mantle **(PM)**, **N-MORB, E-MORB**, and **OIB** values from Sun and McDonough (1989). Symbols are as in figure 4.

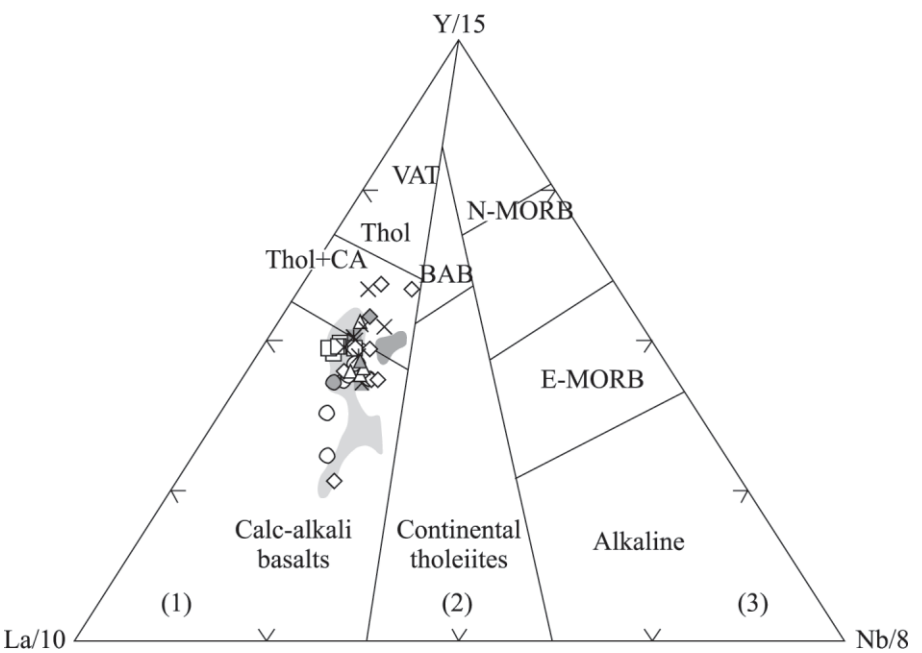

FIG. 10. Tectonic setting discrimination diagram (Cabanis and Lecolle, 1989) for volcanic and (basic-intermediate) plutonic rocks and dike from the Coastal Cordillera of northern Chile. **1-** orogenic domains; **2-** intracontinental and postorogenic domains; **3-** anorogenic domains. **CA**=calc-alkaline basalts; **VAT**= volcanic arc tholeiites; **CB**= continental tholeiites; **BAB**= basalts generated in fore- and back arc basins. Symbols are as in figure 4, shaded areas are as in figure 9.

Gorton and Schandl (2000). In the Iquique area a back-arc setting for the Middle to Upper Jurassic sedimentary and volcanic series has been recognized in a region where the lavas have tholeiitic affinities and bimodal volcanism occurs (Kossler, 1998; Kramer *et al.*, 2005). In this context, the lavas from the Oficina Viz Formation, the oldest unit in this area, are thought to have erupted in a frontal arc position and a westward migration of the arc front has been proposed (Kramer *et al.*, 2005). However, this tectonic setting would have developed only locally, since most of the volcanic and plutonic rocks, with the exception of those in the Oficina Viz Formation studied here, are contemporaneous with the back-arc series described by Kramer *et al.* (2005) (~165-155 Ma) but their geochemical characteristics suggest that they were emplaced in an intra-arc setting.

An extensional to transtensional tectonic regime has been proposed for the development of the magmatic arc in the Coastal Cordillera of northern Chile. A convergent margin dominated by oblique subduction led to strain partitioning, resulting in the development of arc-normal extension and sinistral strike-slip shear zones that would have controlled the magmatic activity and deformation of the arc (Scheuber and González, 1999; Grocott and Taylor, 2002). The fissural volcanism typical for the Coastal Cordillera of northern Chile would have taken place in a weakened trench-parallel sinistral shear zone (Scheuber and González, 1999) or in subsiding intra-arc basins related to arc normal extension in a retreating (low convergence rate) boundary (Grocott and Taylor, 2002). Lower Cretaceous volcanic rocks from the Coastal Cordillera of Central Chile are thought to have extruded also in a setting dominated by subduction and controlled by intra-arc extension due to low-spreading rate of 5 cm yr^{-1} (Åberg *et al.*, 1984; Morata and Aguirre, 2003). These rocks have textural, mineralogical, geochemical and isotopic similarities with the Jurassic volcanic rocks from the Coastal Cordillera of northern Chile, consistent with similar geotectonic conditions.

The short time interval of the volcanic activity relative to the whole magmatic activity of the Jurassic-Early Cretaceous arc in northern Chile (Oliveros *et al.*, 2006) and the relatively homogeneous geochemical character of the volcanic rocks would suggest that a distinctive tectonic setting dominated the continental margin from Middle to Late Jurassic (170 to 150 Ma). During this time, the magmas would have ascended rapidly reaching the surface without major interaction with the continental crust.

CONCLUSIONS

A suite of Middle to Upper Jurassic volcanic and plutonic rocks from the Coastal Cordillera of northern Chile is characterized by chemical and mineralogical homogeneity. The volcanic rocks are highly porphyritic basaltic-andesites and andesites, whereas the intrusive rocks are diorites, granodiorites and granites.

These volcanic and plutonic rocks have calc-alkaline to high-K calc-alkaline affinities, high LILE contents relative to HFSE, Nb-Ta throughs and Ti anomalies, LREE/HREE fractionation and enrichment in Pb over Ce, indicating that they result from subduction-related magmatism. Some differences in trace element patterns between the volcanic and plutonic rocks are explained by chemical differentiation from parental magmas due to plagioclase-olivine-clinopyroxene dominated fractional crystallization.

Assimilation of the continental crust did not play a major role in the evolution of the magmas. However, Th and La content in the studied rocks would indicate increasing sediment contribution or crustal contamination with time. The magma source was likely to have been a depleted mantle metasomatized by slab fluids. No evidence of slab melting involved in the genesis of magmas was found. Finally, the relatively short time interval for volcanism with respect to the whole activity of the arc favoured the extrusion of relatively homogeneous magmas.

ACKNOWLEDGMENTS

This study was supported by the Institut de Recherche pour le Développement (IRD) grant and fellowship. S.M. Kay, J. Cembrano and F. Lucassen are thanked for their helpful reviews which greatly improved the original version of this manuscript.

REFERENCES

Åberg, G.; Aguirre, L.; Levi, B.; Nyström, J.O. 1984. Spreading-subsidence and generation of ensialic marginal basins: an example from the early Cretaceous of central Chile. *In* Marginal Basin Geology (Kokelaar B.P.; Howells M.F.; editors). Geological Society of London, Special Publication 16: 185-193.

Andriessen, P.; Reutter, K. 1994. K-Ar and fission track mineral age determination of igneous rocks related to multiple magmatic arc systems along the 23°S latitude of Chile and NW Argentina. *In* Tectonics of the Southern Central Andes (Reutter, K. J.; Scheuber, E.; Wigger, P.; editors). Springer: 141-153. Heidelberg.

Basso, M. 2004. Carta Baquedano, Región de Antofagasta. Servicio Nacional de Geología y Minería, Carta Geológica de Chile, Serie Geología Básica 82: 26 p., 1 mapa 1:100.000.

Boric, R.; Díaz, F.; Maksaev, V. 1990. Geología y yacimientos metalíferos de la Región de Antofagasta. Servicio Nacional de Geología y Minería, Boletín 40: 246 p., 2 mapas 1:500.000.

Buchelt, M.; Tellez, C. 1988. The Jurassic La Negra Formation in the area of Antofagasta, northern Chile (lithology, petrography, geochemistry). *In* The Southern Central Andes (Bahlburg, H.; Breitkreuz; C.; Giese, P.; editors). Springer, Heidelberg. Lecture Notes in Earth Sciences 17: 171-182.

Büchl, A.; Münker, C.; Mezger, K.; Hofmann, A.W. 2002. High precision Nb/Ta and Zr/Hf ratios in global MORB. Geochimica and Cosmochimica Acta, Abstract, Suppl. 66 A345.

Cabanis B.; Lecolle M. 1989. Le diagramme La/10-Y/15-Nb/8: un outil pour la discrimination des séries volcaniques et la mise en évidence des processus de mélange et/ou de contamination crustales. Comptes Rendus de l'Academie de Sciences de Paris série II 309: 2023-2029.

Cembrano, J.; González, G.; Arancibia, G.; Ahumada, I.; Olivares, V.; Herrera, V. 2005. Fault zone development and strain partitioning in an extensional strike-slip duplex: a case study from the Atacama Fault System, northern Chile. Tectonophysics 400: 105-125.

Cortés, J. 2000. Hoja Palestina, Región de Antofagasta. Servicio Nacional de Geología y Minería, Mapas Geológicos 19, 1 mapa 1:100.000.

Cortés, J.; Marquardt, C.; González, G.; Wilke, H.; Marinovic, N. In press. Carta Mejillones y Península de Mejillones, Región de Antofagasta. Servicio Nacional de Geología y Minería, Carta Geológica de Chile, Serie Geología Básica, 1 mapa 1:100.000.

Dallmeyer, D.; Brown, M.; Grocott, J.; Taylor, G.; Treloar, P.J. 1996. Mesozoic magmatic and tectonic events within the Andean Plate boundary zone, 26°-27°30'S, North Chile: constraints from $^{40}Ar/^{39}Ar$ mineral ages. The Journal of Geology 104: 19-40.

Droop, G.T.R. 1987. A general equation for estimating Fe^{3+} in ferromagnesian silicates and oxides from microprobe analysis, using stoichiometric criteria. Mineralogical Magazine 51: 431-437.

González, G.; Niemeyer, H. 2005. Cartas Antofagasta y Punta Tetas, Región Antofagasta. Servicio Nacional de Geología y Minería, Carta Geológica de Chile, Serie Geología Básica 89: 35, 1 mapa 1:100.000.

Gorton, M.P.; Schandl, E.S. 2000. From continents to island arcs: a geochemical index of tectonic setting for arc-related and within-plate felsic to intermediate volcanic rocks. The Canadian Mineralogist 38: 1065-1073.

Grocott, J.; Taylor, G.K. 2002. Magmatic arc fault systems, deformation partitioning and emplacement of granitic complexes in the Coastal Cordillera, north Chilean Andes (25°30'S to 27°30'S). Journal of the Geological Society of London 159: 425-442.

Hofmann, A.W. 1988. Chemical differentiation of the Earth: the relationship between mantle, continental crust and oceanic crust. Earth and Planetary Science Letters 90: 297-314.

ISC (International Stratrigraphic Chart), 2004. International Commision on Stratigraphy (www.stratrigraphy.org).

Kramer, W.; Siebel, W.; Romer, R.; Haase, G.; Zimmer, M.; Ehrlichmann, R. 2005. Geochemical and isotopic characteristics and evolution of the Jurassic volcanic arc between Arica (18°30'S) and Tocopilla (22°S), North Chilean Coastal Cordillera. Chemie der Erde 65: 47-68.

Klein, E.M.; Karsten, J.L. 1995. Ocean ridge basalt with convergent margin geochemical affinities from the southern Chile Ridge. Nature 374: 52-57.

Kossler, A. 1998. Der Jura in der Küstenkordillere von Iquique (Nordchile): Paläontologie, Lithologie, Stratigraphie, Paläogeographie. Berliner Geowissenschaftliche

Abhandlungen 197 (A).

Jaillard, E.; Soler, P.; Carlier, G.; Mournier, T. 1990. Geodynamic evolution of the northern and Central Andes during early to middle Mesozoic times: A Tethyan model. Journal of the Geological Society of London, 147: 1009-1022.

LeMaitre, R.W. 1989. A classification of igenous rocks and glossary of terms. Blakcwell Scientific Publication: 193 p. London.

Leterrier, J.; Maury, R.C.; Thonon, P.; Girard, D.; Marchal, M. 1982. Clinopyroxene composition as a method of identification of the magmatic affinities of paleo-volcanic series. Earth and Planetary Science Letters 59: 139-154.

Losert, J. 1974. The formation of stratiform copper deposits in relation to alteration of volcanic series (on north Chilean examples). Rezpravy Èeskolovenské Akad. Vìd. Rocnik 84: 1-77.

Lucassen, F.; Franz, G. 1994. Arc related Jurassic igneous and meta igneous rocks in the Coastal Cordillera of Northern Chile/Region Antofagasta. Lithos 32: 273-298.

Lucassen, F.; Fowler, C.M.R.; Franz, G. 1996. Formation of magmatic crust at the Andean continental margin during the early Mesozoic: a geological and thermal model for the north chilean Coast Range. Tectonophysics 262: 263-279.

Lucassen, F.; Thirlwall, M. 1998. Sm-Nd ages of mafic rocks from the Coastal Cordillera at 24°S, northern Chile. Geologische Rundschau 86: 767-774.

Lucassen, F.; Escayola, M.; Romer, R.L.; Viramonte, J.; Koch, K.; Franz, G. 2002. Isotopic composition of Late Mesozoic basic and ultrabasic rocks from the Andes (23-32°S): implication for the Andean mantle. Contributions to Mineralogy and Petrology 143: 336-349.

Lucassen, F.; Kramer, W.; Bartsch, V.; Wilke, H.G.; Franz, G.; Romer, R.L; Dulski, P. 2006. Nd, Pb and Sr isotope composition of juvenile magmatism in the Mesozoic large magmatic province of northern Chile (18-27°): indications for a uniform subarc mantle. Contributions to Mineralogy and Petrology 152: 571-589.

Maksaev, V. 1990. Metallogeny, geological evolution and thermochronology of the Chilean Andes between latitudes 21° and 26° south, and the origin of the major porphyry copper deposits. Ph.D. Thesis (Unpublished), Dalhousie University: 554 p.

Morata, D.; Aguirre, L. 2003. Extensional Lower Cretaceous volcanism in the Coastal Range (29°20'-30°S), Chile: geochemistry and petrogenesis. Journal of South American Earth Sciences 16: 459-476.

Morimoto, N.; Fabrics, J.; Ferguson, A. K.; Ginzburg, I. V.; Ross, N.; Seifert, F. A.; Zussman, J.; Aoki, K.; Gottardi, G. 1988. Nomenclature of pyroxenes. Mineralogical Magazine 52: 535-550.

Mpodozis, C.; Ramos, V. 1989. The Andes of Chile and Argentina. *In* Geology of the Andes and its relation to hydrocarbon and mineral resources (Ericksen, G.E.; Cañas Pinochet; M.T.; Reinemund, J.A.; Editors). Houston, Texas, Circum-Pacific Council for Energy and Mineral Resources, Earth Sciences Series 11: 59-90.

Münker, C.; Pfänder, J.A.; Weyer, S.; Büchl, A.; Kleine, T.; Mezger, K. 2003. Evolution of planetary cores and the Earth-Moon system from Nb/Ta systematics. Science 301: 84- 87.

Muñoz, N.; Venegas, R.; Tellez, C. 1988. La Formación La Negra: Nuevos antecedentes estratigráficos en la Cordillera de la Costa de Antofagasta. *In* Congreso Geológico Chileno, No. 5, Actas 1: A283 - A311.

Oliveros, V.; Aguirre, L.; Townley, B. 2003. Alteration processes in igneous rocks of the Michilla mining area, Coastal Range, northern Chile, and their relation with copper mineralisation. E.G.S. XXVII, 4 ed., European Geophysical Society (ed.), Geophysical Research Abstracts, Nice: 383.

Oliveros, V. 2005. Etude Géochronologique des Unités Magmatiques Jurassiques et Crétacé Inférieur du Nord du Chili (18°30'-24°S, 60°30'-70°30'W): Origine, Mise en Place, Altération, Métamorphisme et Minéralizations Associées. Unpublished Ph.D. Thesis. University of Nice-University of Chile.

Oliveros, V.; Féraud, G.; Aguirre, L.; Fornari, M.; Morata, D. 2006. The Early Andean Magmatic Province (EAMP): $^{40}Ar/^{39}Ar$ dating on Mesozoic volcanic and plutonic rocks from the Coastal Cordillera, Northern Chile. Journal of Volcanology and Geothermal Research 157: 311-330. doi:10.1016/j.jvolgeores.2006.04.007

Oliveros, V.; Féraud, G.; Aguirre, L.; Ramírez, L.E.; Palacios, C.; Fornari, M.; Parada, M.A. In press(a). The Late Jurassic Mantos Blancos major copper deposit, Coastal Range, northern Chile: $^{40}Ar/^{39}Ar$ dating of two overprinted magmatic-hydrothermal breccia-feeding mineralization events. Mineralium Deposita.

Oliveros, V.; Tristá, D.; Féraud, G.; Morata, D.; Aguirre, L.; Kojima, S. In press(b). Time-relationships between volcanism-plutonism-alteration in Cu-stratabound ore deposits: the Michilla district, northern Chile. A $^{40}Ar/^{39}Ar$ geochronological approach. Mineralium Deposita.

Palacios, C. 1978. The Jurassic paleovolcanism in northern Chile. Ph.D. Thesis (Unpublished), Tubingen University: 99 p.

Pearce, J.A. 1982. Trace elements characteristics of lavas from destructive plate boundaries. *In* Andesites (Thorpe R.S.; Editor). John Wiley and Sons: 525-548. London.

Pearce, J.A. 1983. Role of sub-continental lithosphere in magma genesis at active continental margins. *In* Continental Basalts and Mantle Xenoliths (Hawkesworth, C.J.; Norry M.J.; Editors). Shiva: 203-249. Chesire.

Peate, D.W.; Pearce, J.A.; Hawkesworth, C.J.; Colley, H.; Edwadrs, C.M.H.; Hirose, K. 1997. Geochemical

variations in Vantu arc lavas: the role of subducted material and a variable mantle wedge composition. Journal of Petrology 38: 1331-1358.

Pichowiak, S.; Buchelt, M.; Damm, K.W. 1990. Magmatic activity and tectonic setting of early stages of Andean cycle in northern Chile. Geological Society of America, Special Paper 241: 127-144.

Pichowiak, S. 1994. Early Jurassic to Early Cretaceous magmatism in the Coastal Cordillera and the Central Depression of North Chile. *In* Tectonics of the Southern Central Andes (Reutter, K.J.; Scheuber, E.; Wigger, P.; Editors). Springer: 203-217. Heidelberg.

Plank, T. 2005. Constraints from Thorium/Lanthanum on sediment recycling at subduction zones and the evolution of continents. Journal of Petrology: 46: 921-944.

Prinz, P.; Wilke, H.G.; von Hillebrandt, A. 1994. Sediment accumulation and subsidence history in the Mesozoic marginal sea in N-Chile. *In* Tectonics of the Southern Central Andes (Reutter, K. J.; Scheuber, E.; Wigger, P.; Editors). Springer: 219-233. Heidelberg.

Rickwood, P.C.1989. Boundary lines within petrologic diagrams which use oxides of major and minor elements. Lithos 22: 247-263.

Rogers, G. 1985. A geochemical traverse across the north chilean Andes. Ph.D. Thesis (Unpublished), Open University, 333 p.

Rogers, G.; Hawkesworth, C.J. 1989. A geochemical traverse across the North Chilean Andes: Evidence for crust generation melt from the mantle wedge. Earth and Planetary Science Letters 91: 271-285.

Russell, J.K.; Nichols, J. 1988. Analysis of petrologic hypotheses with Pearce element ratio. Contributions to Mineralogy and Petrology 99: 25-35.

Scheuber, E.; Hammerdschimdt, K.; Frieddrischen, H. 1995. ^{40}Ar-^{39}Ar and Rb-analyses from ductile shear zones from the Atacama Fault Zone, northern Chile: the age of deformation. Tectonophysics 250: 61-87.

Scheuber, E.; González, G. 1999. Tectonics of the Jurassic-Early Cretaceous magmatic arc of the north Chilean Coastal Cordillera (22°-26°S): A story of crustal deformation along a convergent plate boundary. Tectonics 18: 895-910.

SERNAGEOMIN 2002. Mapa Geológico de Chile. Servicio Nacional de Geología y Minería, Chile. Carta Geológica de Chile, Serie Geología Básica 75, 1 mapa en 3 hojas, 1:1.000.000.

Sun, S. -s; McDonough, W.F. 1989. Chemical and isotope systematics of oceanic basalts: implications for mantle composition and processes. *In* Magmatism in the Ocean Basins (Saunders, A.D; Norry, M.J; editors). Geological Society, London, Special Publications 42: 313-345.

Wedepohl, K.H. 1995. The composition of the continental crust. Geochimica and Cosmochimica Acta 59: 1217-1232.

Winchester, J.A.; Floyd, P.A. 1977. Geochemial discrimination of different magma series and their differentiation products using immobile elements. Chemical Geology 20: 325-343.

Manuscript received: May 29, 2006; accepted: April 3, 2007.